THERMODYNAMIC ACTIVITIES OF SOLID BETA SILVER-ZINC ALLOYS

by

ERVIN E. UNDERWOOD

B. S., Purdue University

(1949)

Submitted in Partial Fulfillment of the Requirements

for the Degree of

MASTER OF SCIENCE

from the

Massachusetts Institute of Technology
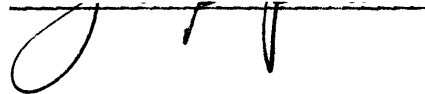
(1951)

Signature of Author
 Department of Metallurgy
 May 18, 1951

Signature of Professors
 in Charge of Research

Signature of Chairman,
 Department Committee on
 Graduate Students

## ABSTRACT

Thermodynamic Activities of Solid Beta Silver-Zinc Alloys

Ervin E. Underwood

Submitted for the degree of Master of Science
in the Department of Metallurgy on May 18, 1951

Using the dew point method, vapor pressures of zinc over solid silver-zinc alloys have been determined over a temperature range of 525–660° C for compositions of 43.4, 50.3 and 53.7 atomic percent zinc.

Zinc vapor pressures have also been measured for –325 mesh silver-zinc filings of the same compositions. A 16–19 percent increase in vapor pressure of as-filed powders over that from the corresponding solid alloy was obtained, but the preheated powders did not show this increase.

3.33 and 6.68 atomic percent gold was added to silver-zinc alloys making ternary alloys with 47.8 and 43.9 atomic percent zinc respectively. Activities were calculated over a temperature range of 500–660° C. At 620° C the activities of zinc in the ternary alloys were 16.5 percent and 11.0 percent less than those of the corresponding binary alloys.

The vapor pressures of zinc in equilibrium with the (100), (110) and (111) planes of silver-zinc single crystals, of 50.7 atomic percent zinc, were measured over a temperature range of 540–640° C. Although slight differences were noted, no conclusions could be drawn since the deviations were within the experimental error.

# TABLE OF CONTENTS

# LIST OF FIGURES

## LIST OF TABLES

# ACKNOWLEDGMENTS

It is a genuine pleasure to acknowledge the inspiration and stimulation, both professional and personal, afforded by association with Professor Morris Cohen during this project.

Many thanks are due Professor B. L. Averbach for directing the course of this research, and for his careful editing and invaluable criticisms of the thesis.

The unfailing generosity of Mr. Leslie L. Seigle with his many suggestions, his encouragement, and his time is gratefully acknowledged here.

Among many others who were unsparing with helpful counsel may be listed Mr. Nils Christensen, Mr. Earl C. Roberts, Mr. Paul A. Flinn and Mr. Donald A. Hay.

A special word of thanks is extended to my wife, Marlit, who typed the thesis under unusually confining conditions, and made its completion possible.

The silver-zinc single crystal was kindly provided by Professor B. E. Warren; the chemical analyses were performed by Mr. W. M. Saunders and Mr. D. L. Guernsey.

This research was sponsored in part by the Atomic Energy Commission under Contract No. AT-30-1-GEN-368.

## I. INTRODUCTION

The vapor pressures of zinc in solid silver-zinc alloys have been measured over a range of temperatures near the composition AgZn in order to calculate the activities of the two components. A knowledge of the activities will enable other thermodynamic properties to be calculated, and as x-ray measurements of short range order are made, a correlation between the local order and the thermodynamic properties may appear.

There are additional features of interest in these compositions near 50 atomic percent zinc. The disordered body-centered cubic structure present at high temperatures undergoes a transformation near 280° C. Upon slow cooling a complex hexagonal structure, the Zeta phase, is formed. On quenching from above 280° C, however, an ordered CsCl-type structure is obtained. The ordering reaction is of the $\beta$ -brass type and the disordered phase cannot be obtained at room temperature on quenching. If the ordered alloy is heated below 280° C the complex Zeta structure is formed. It is thus impossible to study the order-disorder reaction in the binary AgZn alloy.

This research applied Hargreaves' dew point method of measuring vapor pressures over solid alloys[1] and, except for a few modifications, the same experimental arrangements. This method can be used provided one component is appreciably more volatile than the other. It is also necessary that the vapor pressures be greater than one millimeter of mercury, so that clearly visible droplets of the pure volatile

constituent can be made to condense at certain temperatures within a reasonable amount of time.

The solid alloy, at some constant temperature, $T_h$, has a certain vapor pressure of zinc. When the alloy is enclosed in an evacuated tube, droplets of zinc can be made to condense at the other end by lowering the temperature there. By a judicious evaporation and condensation of these droplets, the value of $T_c$ — the equilibrium temperature between gaseous and liquid zinc — can be established as lying within a small temperature interval. Knowing this temperature permits the calculation of the zinc vapor pressure within the tube, i.e. the vapor pressure of zinc over the alloy.

The vapor pressures of zinc in equilibrium with three silver-zinc polycrystalline alloys were obtained. Using the same experimental method, vapor pressures were also measured for -325 mesh silver-zinc filings, from silver-zinc plus gold ternary alloys, and from different faces of AgZn single crystals.

It was hoped that a particle size effect on the vapor pressure could be detected from the filings. According to the well-known Thompson equation[20]

$$\ln \frac{p'}{p} = \frac{2\sigma M}{RT\rho}\left(\frac{1}{r}\right) \tag{1}$$

where  $p'$ = the vapor pressure over a curved surface

$p$ = the vapor pressure over a flat surface

$\sigma$ = the surface tension

$M$ = the molecular weight

$R$ = the gas constant

T = the temperature, $^\circ$K

$\rho$ = the density

r = the radius of curvature of the curved surface

the vapor pressure, p', of a small liquid droplet should increase as its radius, r, decreases. An order of magnitude calculation using $\sigma \approx 700$ dynes per centimeter at 800$^\circ$ K for zinc droplets of radius $r \approx 0.002$ centimeter, shows that the ratio of $p'/p \approx 1.0001$. For solid silver-zinc particles an even smaller difference would be expected. Only under extremely difficult experimental conditions was it possible to detect an effect, and this without a high degree of certainty.

The addition of gold to silver-zinc alloys resulted in a decrease of the zinc vapor pressure -- an effect similar to that noted by Hargreaves[1] when nickel was added to copper-zinc alloys. In the present case, it was hoped that the same success in correlating x-ray and thermodynamic data could be obtained as with the gold-silver system[2]. Using the results of a recent x-ray determination of long-range ordering in silver-zinc alloys[3], various calculations have been made to find the extent of agreement between data from both methods.

The measurement of zinc vapor pressures from different crystallographic planes of a AgZn single crystal showed small but consistent differences. These differences were, however, within the experimental error.

In a rather striking experiment, Mehl and McCandless[4] showed definite and reproducible differences in the rate of oxide film formation on single crystals of iron. R. P. Johnson[5] observed a tendency

in incandescent wolfram wires heated with alternating current, to
expose smooth concave (110) faces when in a neutral gas. These seem-
ingly diverse phenomena indicate distinctive properties for certain
crystallographic faces but these effects were not observed here.
However, this research was concerned with equilibrium conditions, and
not rate effects.

## II. LITERATURE SURVEY

Wagner[6], Chipman and Elliott[7], and Seigle and Turnbull[8] have published extensive bibliographies of the literature dealing with the determination of activities. The dew point method of vapor pressure measurement has been described by Hargreaves[1], and Weibke and Kubaschewski[10] have presented an excellent general text on the thermochemistry of alloys. The determinations by Birchenall and Cheng[9] of the vapor pressures of zinc over solid silver-zinc alloys were directly related to the present work, and Schneider and Schmid[11] have measured the vapor pressures over liquid silver-zinc alloys using Hargreaves' experimental arrangements.

Most of the papers dealing with the effect of particle radius on vapor pressure have concerned themselves with either theoretical derivations or inconclusive experimental results. However, Bigelow and Trimble[12], in an impressive attempt to obtain a quantitative verification of the J. Thompson equation, concluded that the effects are so small as to be obliterated by other phenomena.

Books by Adam[13] and Rideal[14] cover the physics and chemistry of surfaces and discuss some aspects of the solubility of small particles; Shuttleworth[15] and Koenig[16] deal with theoretical thermodynamic aspects of surface tension and curvature; while oft-quoted experimental work on the solubility of small particles are those of Ostwald[17], Hulett[18], and Freundlich[19].

A recent paper by Muldawer[3] gives information on long-range order in silver-zinc alloys obtained by x-ray methods which should be amenable to confirmation by suitable thermodynamic data. References are made to correlation of x-ray data with that obtained by thermodynamic means by Birchenall[2] and also by Wagner[6].

No recent literature was found dealing with the vapor pressure occurring from different faces of a single crystal, although several books and articles on crystal growth were consulted. Buckle[23] wrote an article on diffusion through noble-metal plating and gave an approximate value of the diffusion constant of zinc in silver. An article by Larke and Wicks[25] pointed the way to a satisfactory electrolytic etch for the AgZn single crystals.

## III. MATERIALS AND EQUIPMENT

### A. Metals Used for Alloying

The silver shot (obtained from Handy and Harman Company) used in making up the alloys was about 999.9+ fine, with traces of copper and iron. Zinc sticks of analytical reagent grade were used, with a maximum limit of impurities of not more than 0.01 percent iron, arsenic, or lead. For the ternary alloys, 0.020 inch diameter gold wire, 999.7 fine with the balance consisting of copper and silver, or gold shot with 99.96 percent gold, 0.03-0.04 percent silver and traces of copper, palladium and iron (also from Handy and Harman Company), were used.

### B. Furnace and Controls

A modified version of Hargreaves'[1] furnace was employed for the dew point measurements. The furnace tube was heated by three main resistance windings, with an auxiliary coil to heat the side tubes for the observation windows. A small coil, independently controlled, was placed around the condensation end of quartz tube for fine temperature control. A sketch of the furnace details is shown in Figure 1.

The current in each of the furnace coils was controlled independently by four Variacs, and a Foxboro potentiometer controller was used to maintain a constant temperature at the sample end of the furnace. The maximum variation observed was about ±1° C occurring over a five minute cycle. A typical temperature gradient along the furnace tube is shown in Figure 2.

CONTROL
THERMOCOUPLE
TUBE

SIL-O-CEL
PACKING

TELESCOPE

TRANSITE

FURNACE
COILS

AUXILIARY
COILS

END
PLUG

ALUNDUM
TUBES

SPECIMEN

QUARTZ TUBE

BINDING POSTS

STAINLESS STEEL
SHELL

LAMP
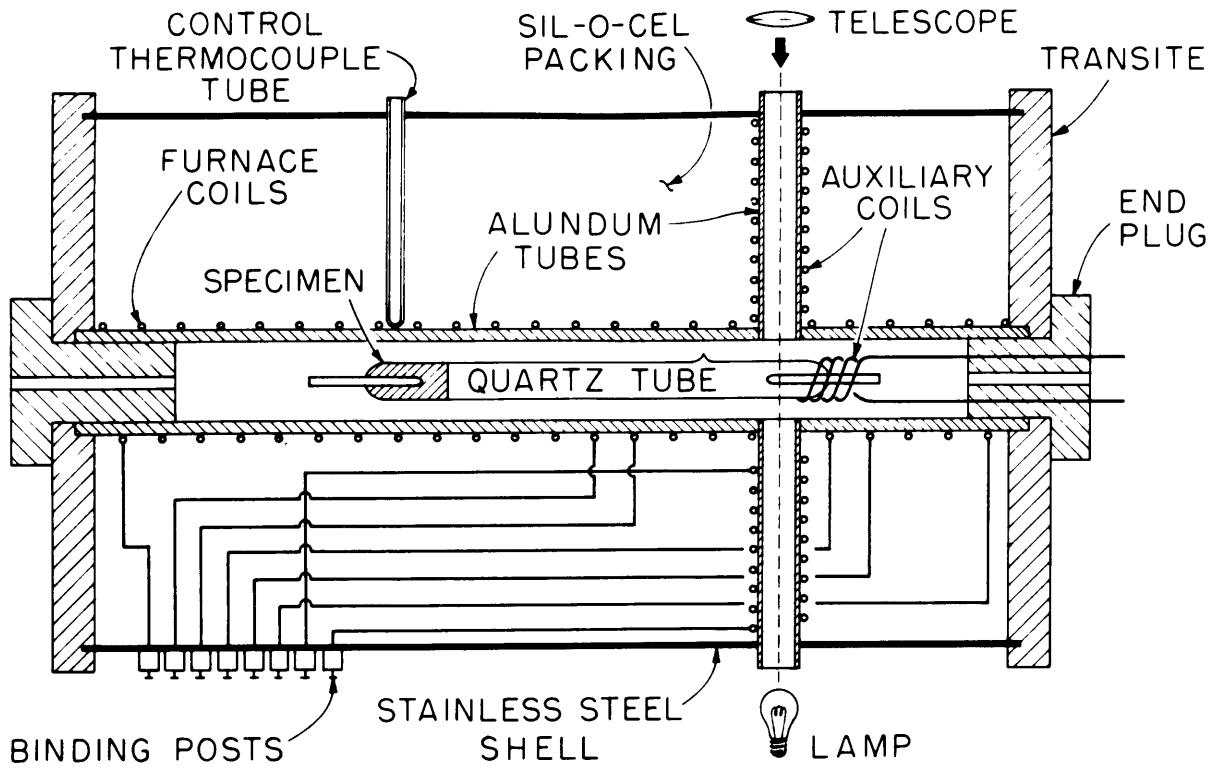
SKETCH OF FURNACE CROSS-SECTION
FIGURE 1

POSITION OF
SPECIMEN

LOCATION
OF DEPOSIT

T (°C)

DISTANCE (INCHES)
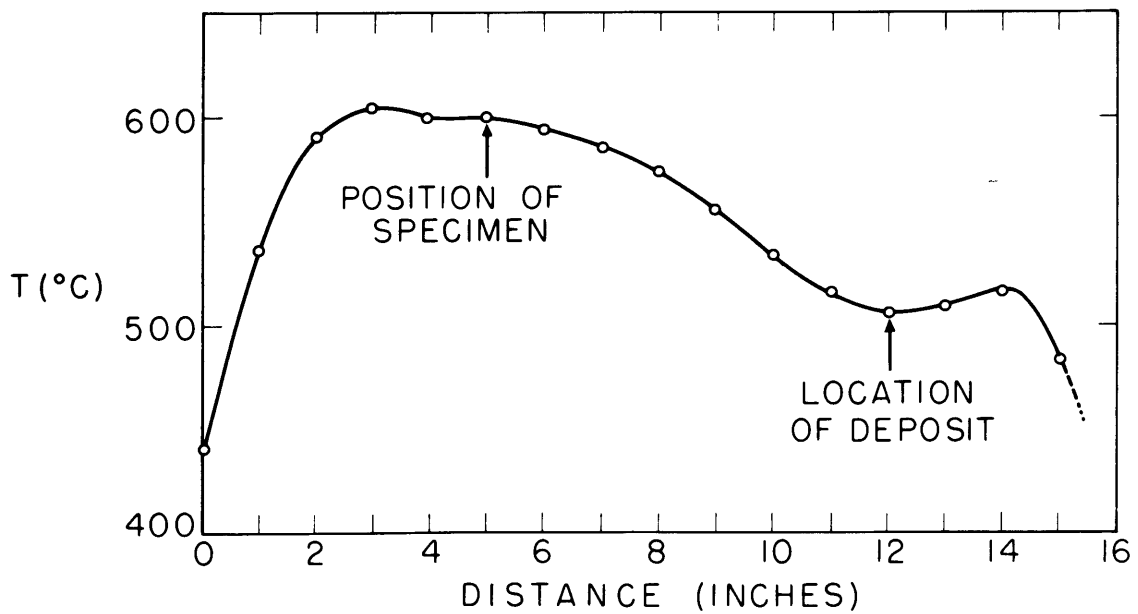
TEMPERATURE GRADIENT ALONG FURNACE TUBE
FIGURE 2

## C. Specimen Tubes

Clear quartz specimen tubes with side arms for evacuation and sealing were used. Thermocouple wells were introduced at both ends in order to allow the thermocouple beads to rest within the tube, close to the deposit and the specimen. The tubes were evacuated to less than $10^{-1}$ millimeter of mercury and the vacuum was tested with a spark coil.

## D. Miscellaneous Equipment

Thermocouples were made from 0.026 inch Chromel-Alumel wires, and these were calibrated against a platinum-platinum ten percent rhodium thermocouple. This in turn had been compared with a platinum-platinum ten percent rhodium thermocouple calibrated at the Bureau of Standards.

A Cenco reading telescope with a maximum magnification of ten times was used to observe the condensation and evaporation of the zinc droplets.

The potentiometer used to measure the temperatures of the alloy specimens and droplets was a Rubicon portable precision potentiometer. It was checked both at the factory and with a recently calibrated leeds and Northrup type 8662 potentiometer. Both potentiometers agreed over a temperature range of 425-840° C within 0.01 millivolt.

## IV. POLYCRYSTALLINE BINARY ALLOYS

### A. Preparation of Specimens

Pure silver was melted in graphite crucibles in an induction furnace. Zinc sticks were added quickly during stirring, with an allowance being made for volatilization losses. The crucible and melt were quenched into water within a few minutes after all the zinc had been added.

The cylindrical ingot was machined from 1 1/8 inches diameter to about 3/4 inch to remove oxides. Then specimens were annealed for several days at 640° C in an evacuated Vycor container and quenched.

The homogenized slug was then machined to final dimensions— 3/8 inch diameter by 1 1/16 inches long — and a 7/32 inch diameter hole was drilled about 1/2 inch into one end so that the specimen would slip over the quartz tube thermocouple well. The surface of the specimen was smoothed with 000 emery paper and cleaned in benzene. The final weight of the specimens averaged about 12 grams.

The specimens were then sealed off in the clear quartz tubes which had been degreased in cleaning solution. The tube was evacuated, hydrogen gas was flushed through, and the evacuation was repeated. The final pressure obtained was less than $10^{-1}$ millimeter of mercury.

### B. Procedure

The specimen in its quartz tube was placed into the furnace so that the condensation end of the tube could be seen. The Chromel-

Alumel thermocouples were then inserted into the thermocouple wells at the ends of the tube, the automatic controller set at the desired temperature, and the specimen left to heat overnight.

The next morning the run was begun by slowly lowering the temperature of the tube at the observation end of the furnace. After a definite deposit of zinc droplets was observed, further temperature control was made by means of the fine adjustment auxiliary coil around the tube at the cold end. In many cases the initial deposit did not appear directly in front of the observation window due to improper heat distribution in the main coils. However, by a judicious shifting of currents in the windings, the deposit could be moved to the desired vantage point.

The temperature of the cold end was then raised slightly by the auxiliary coil until the droplets had evaporated, the cycle of condensation and evaporation being repeated more slowly as the temperatures approached one another. This "bracketing" was continued until the smallest feasible limit consistent with that temperature was obtained. At the higher temperatures a $2^{\circ}$ C bracket could be obtained readily while at lower temperatures a $3-5^{\circ}$ C bracket could not be narrowed even after prolonged holding at intermediate temperatures. A two-hour period was needed to establish a $4-5^{\circ}$ C bracket at about one millimeter zinc vapor pressure, while 5-10 minutes were quite adequate at zinc vapor pressures of 15 millimeters.

The temperature at which the Zn ($\ell$) = Zn (g) equilibrium existed was taken as halfway between the final temperatures of condensation and

evaporation. This temperature is referred to as $T_c$ (for the cold end).

In general, runs were made at seven different temperatures for each alloy, and were staggered (3, 7, 2, ... etc.) so that any systematic errors could be detected.

Chemical analyses were made from machinings from the homogenized cylinder before the run. Afterwards, chips for analysis were obtained by sawing through the middle of the specimen. Excellent agreement was obtained using these different sampling techniques (see Table I) showing that very little zinc had been lost during the runs and that homogenization had been accomplished.

TABLE I

Chemical Analyses of Binary Alloys
(Weight percent)

Before vapor pressure measurements:

| Ag: | 68.32 | 62.10 | 58.80 |
|-----|-------|-------|-------|
| Zn: | 31.80 | 38.16 | 41.36 |
|     | 100.12 | 100.26 | 100.16 |

After vapor pressure measurements:

| Ag: | 67.55 | 62.21 | 58.83 |
|-----|-------|-------|-------|

C. Discussion of Results

for a quick and convenient correlation of the experimental values as the runs progressed, advantage was taken of the straight line relationship between $1/T_h$ and $1/T_c$.

For a horizontal tube of the dimensions used, at the temperature range involved, and at the pressures encountered, the pressure throughout a tube heated unequally at the ends could be considered the same. Thus, from the Clausius-Clapeyron equation[20], we have

$$\ln p_h = -\frac{\Delta H}{R T_h} + C \tag{2}$$

and

$$\ln p_c = -\frac{\Delta H}{R T_c} + C' \tag{3}$$

where  $p_h$ = pressure of zinc at the hot end of the tube

$p_c$ = pressure of zinc at the cold end of the tube

$\Delta H$ = heat of vaporization of Zn

R = gas constant

$T_h$ = temperature at the hot end, °K

$T_c$ = temperature at the cold end, °K

C = integration constant

C' = integration constant.

Since at equilibrium $p_h = p_c$,

$$-\frac{\Delta H}{R T_h} + C = -\frac{\Delta H}{R T_c} + C' \tag{4}$$

or

$$1/T_h = K \cdot 1/T_c + K' \tag{5}$$

assuming $\Delta H$, C and C' constant over the temperature range (160° C).

Figure 3 shows the plot of the experimental temperature values, (which are also tabulated in Table VI in the Appendix) with the best straight line through them determined by the method of least squares. Values of $1/T_h$ and $1/T_c$ were determined at 20° C intervals from the
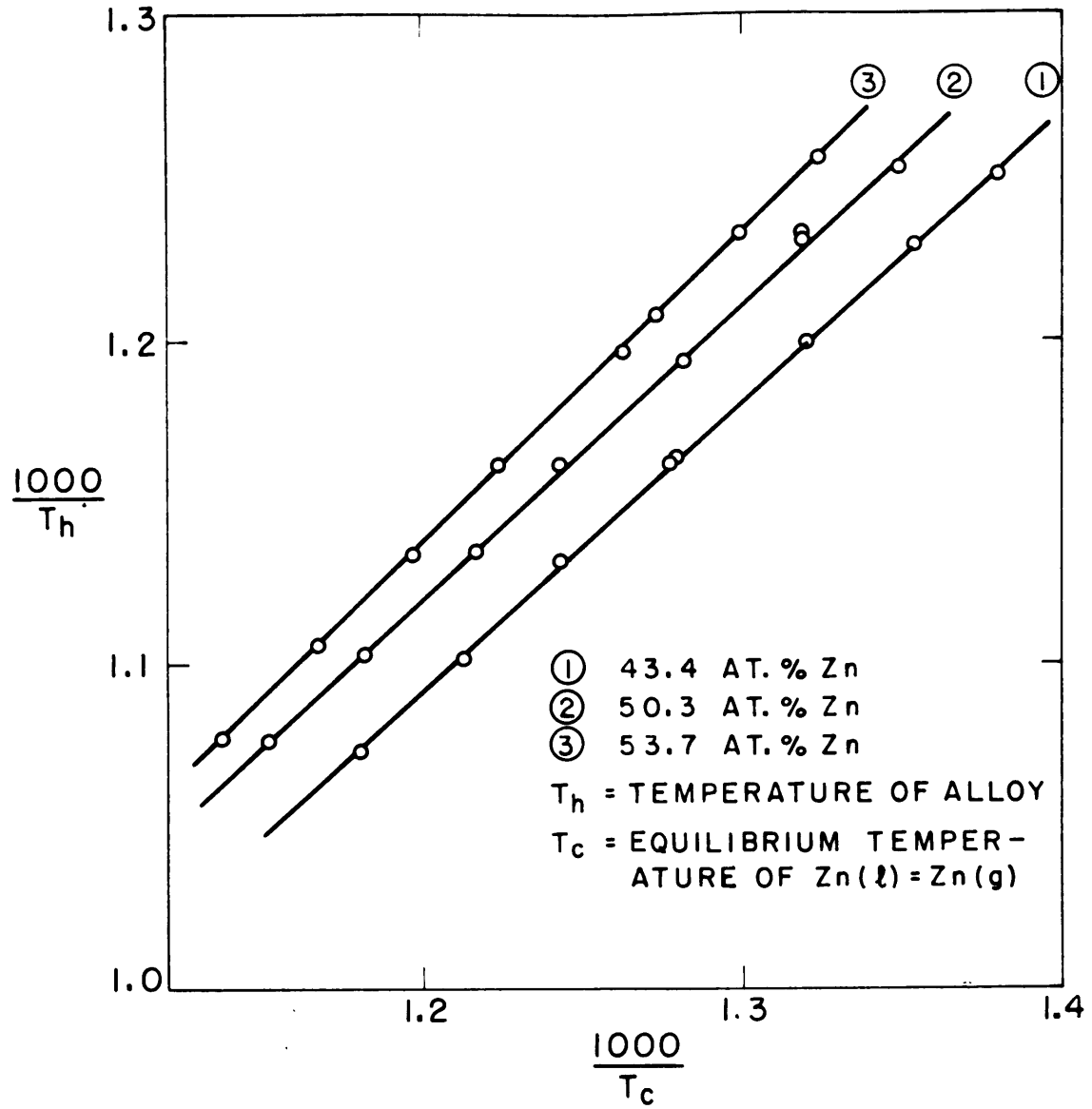
PLOT OF $\frac{1}{T_h}$ VS $\frac{1}{T_c}$ FOR BINARY ALLOYS

FIGURE 3

equation of this line in order to minimize the scatter in the subsequent calculations.

The equations of K. K. Kelley[21] relating the vapor pressure of pure zinc with its temperature were employed to determine the vapor pressures of zinc. Fortunately this empirical equation for zinc vapor pressures represents the actual data extremely well over the entire temperature range of this investigation. Activities were calculated by substituting the temperatures obtained at 20° C intervals from the lines in Figure 3 into the free energy equation

$$\Delta F^O = 30,902 + 6.03T \log T + 0.275 \times 10^{-3}T^2 - 45.03T \qquad (6)$$

to get the pressures corresponding to $\Delta F^O = -RT \ln p_{Zn}$.

Since at equilibrium the partial pressure of zinc over the alloy at $T_h$ equals the vapor pressure of zinc over the pure liquid droplets at $T_c$, the partial pressure of zinc over the alloy at $T_h$ is found by evaluating Equation 6 at $T_c$. Therefore the activity of zinc in the solid alloy with respect to pure liquid zinc at the same temperature becomes

$$a(\text{Zn in alloy at } T_h) \equiv \frac{P(\text{Zn vapor over liquid Zn at } T_c)}{P(\text{Zn vapor over liquid Zn at } T_h)} \qquad (7)$$

Activity values obtained in this manner are shown in Figure 4 on the silver-zinc equilibrium diagram as given in the Metals Handbook[22]. A tabulation of activity and activity coefficients of zinc is made in Tables XIV and XV in the Appendix.

Inasmuch as the thermocouple bead was placed at the center of the quartz tube but the zinc droplets were condensing on the outer
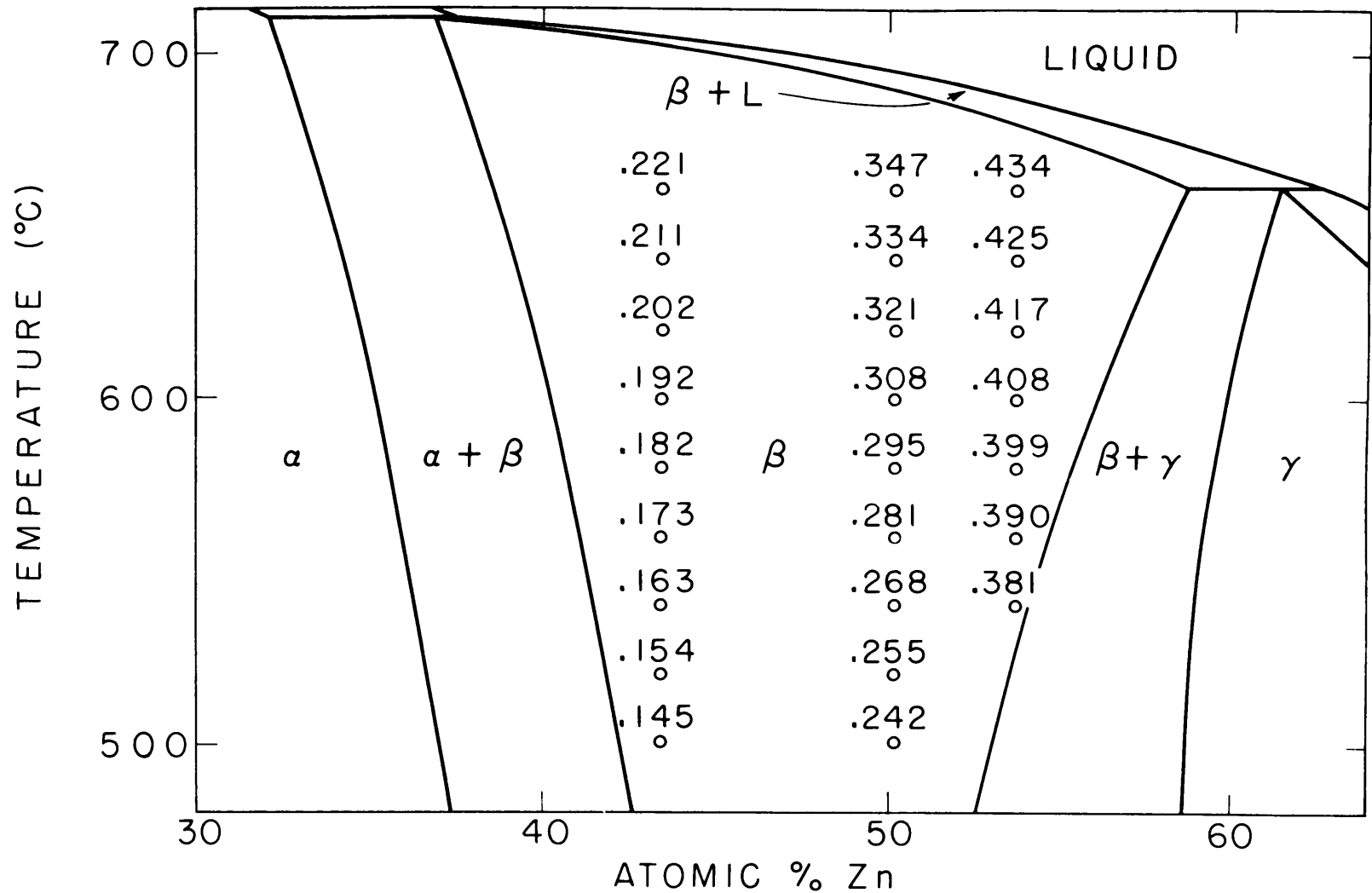
ACTIVITIES OF Zn ON THE Ag – Zn EQUILIBRIUM DIAGRAM
(REFERRED TO LIQUID Zn)
FIGURE 4

wall, a measurement of the temperatures at the two points was made. An average temperature difference of 1.9° C was obtained (colder on the outside) — both with the two thermocouples placed one way, and then switched. This error was minimized by causing the deposit to form slightly to the right of the bead at a point where the temperature was approximately 2° less than that over the bead. A one degree error in $T_c$ was found to introduce a relative error of 2.4 percent in the activity of zinc in an alloy of 43.4 atomic percent zinc at 580° C. This value may be considered as representative of the order of the errors involved. Deviations in chemical analyses averaged between 1-2 percent.

Schneider and Schmid[11] estimated an average relative error of $\pm$ 3 percent in calculating activities. Birchenall and Cheng[9], in an excellent analysis of the possible errors, arrived at 10 percent for their over-all error, which is also a reasonable figure for this research.

Comparison of the present results with an interpolation of Birchenall and Cheng's data[9] at 620° C shows a gradually increasing discrepancy across the $\beta$-field as the zinc content increases (see Figure 5). The reason for this difference is difficult to deduce because good agreement was obtained at one composition in the $\alpha$-field. It is possible that the construction of Birchenall and Cheng's furnace, which apparently would not permit much lateral movement of the tube in the furnace, might be responsible for this discrepancy in activity values. Sometimes the zinc droplets would condense initially out of
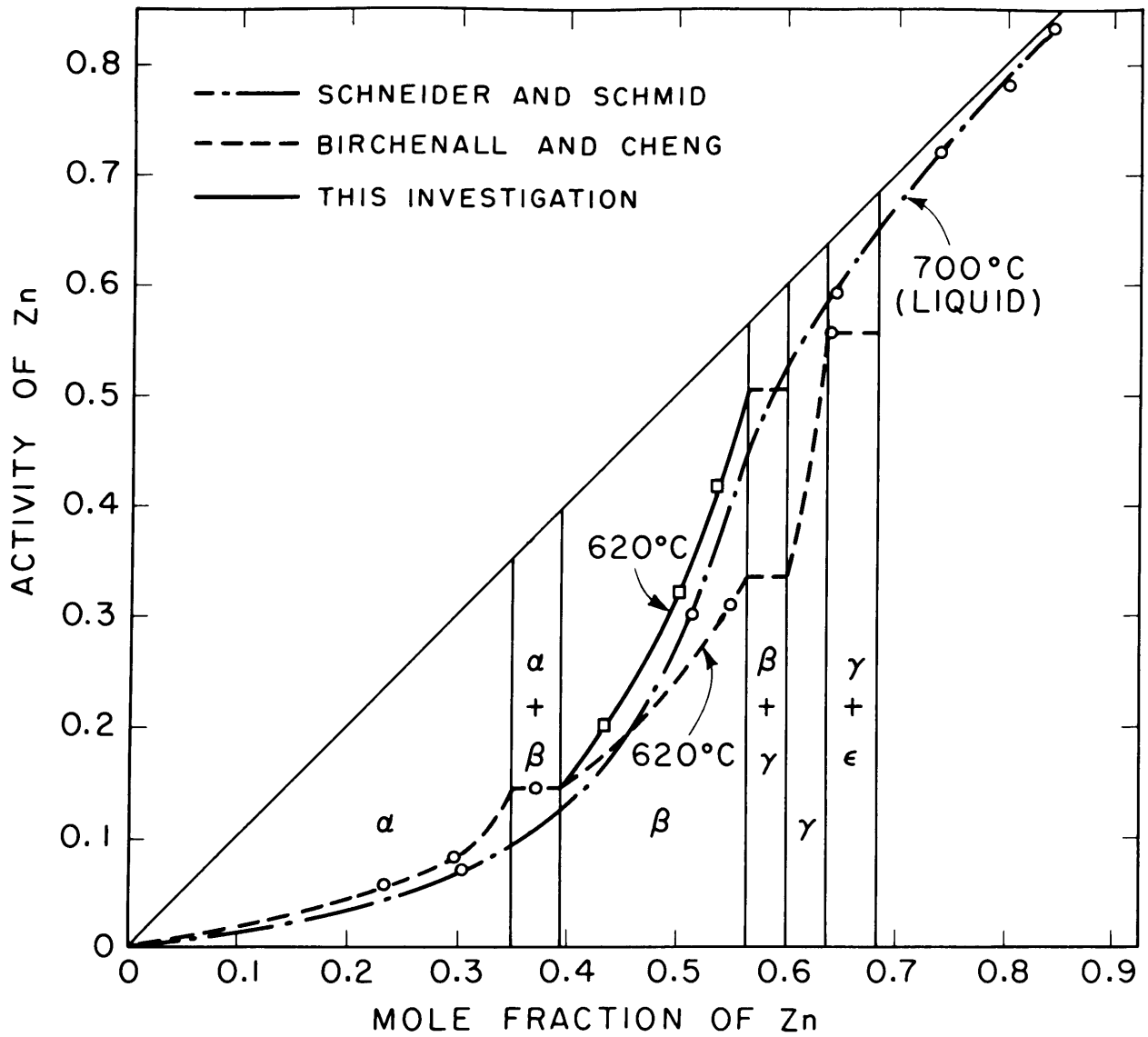
ACTIVITY OF Zn IN AgZn ALLOYS AT 620°C
(REFERRED TO LIQUID Zn)

FIGURE 5

view, and it would not be until lower temperatures had been attained that the spreading deposit could be noted. The fact that condensation tended to start at the same spot, even at the different temperatures, would appear to bolster this explanation.

A check run at one temperature for each composition was made with a different potentiometer, and the original data were verified in each case. It is of interest to note that the superposition of Schneider and Schmid's[11] activity values for liquid alloys at 700° C shows a striking similarity to the present data for solid alloys (Figure 5).

In order to compare Schneider and Schmid's data[11] with this research, extrapolations were made to the liquidus and solidus. Their activity values at 700° C give the activity of zinc at the liquidus as about 0.24 while an extrapolation of zinc activities in the solid alloys to the solidus at 700° C gives a value of activity of zinc equal to 0.26. In this range of compositions the activity of zinc varies rapidly with composition, therefore such a comparison may be subject to some uncertainty.

Partial molar heats of formation were calculated for the three compositions from plots of $\ln a$ vs. $1/T_h$ and are tabulated in Table XVII in the Appendix. A comparison of partial molar heats of mixing for liquid, and partial molar heats of formation for solid silver-zinc alloys as obtained from papers by Schneider and Schmid[11], Birchenall and Cheng[9] and from this work shows some interesting features (see Figure 6).
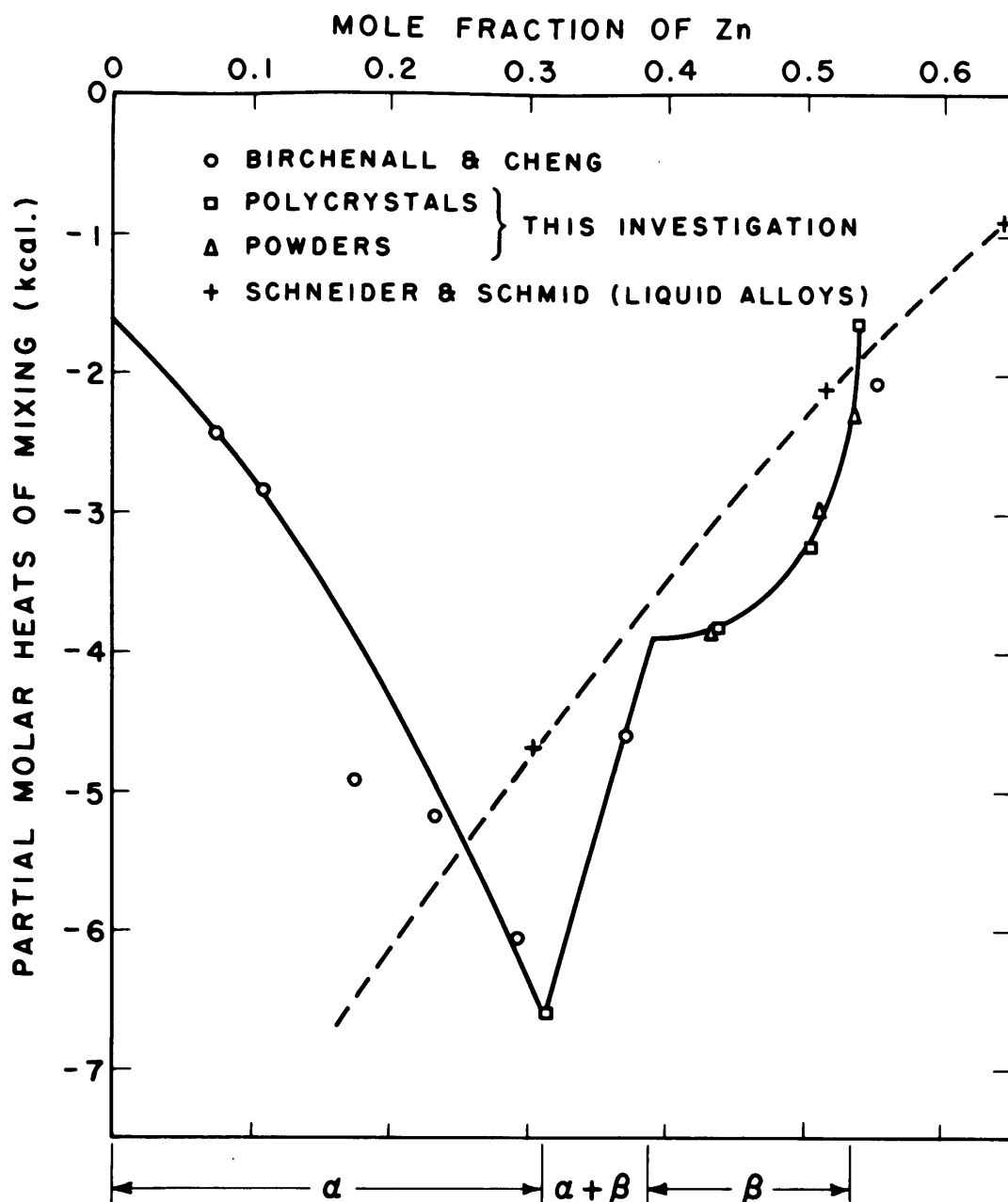
PARTIAL MOLAR HEATS OF FORMATION
FOR Ag-Zn ALLOYS

FIGURE 6

Although the extensive data of Schneider and Schmid at $775^{\circ}$ C show a smooth and continuous increase of $\Delta \bar{H}$ with increasing zinc composition, this is not the case for the solid alloys. Considering the extreme sensitivity of $\Delta \bar{H}$ values to small changes in slope, excellent agreement is shown in the $\beta$-field between the polycrystalline and powder specimens.

Using the Gibbs-Duhem equation, the activities of silver have been calculated at $620^{\circ}$ C and are plotted in Figure 7. The activity coefficients given by Birchenall and Cheng[9] were used in the $\alpha$-field. The activities and activity coefficients of silver at $620^{\circ}$ C in silver-zinc alloys are tabulated in Table XVI in the Appendix.
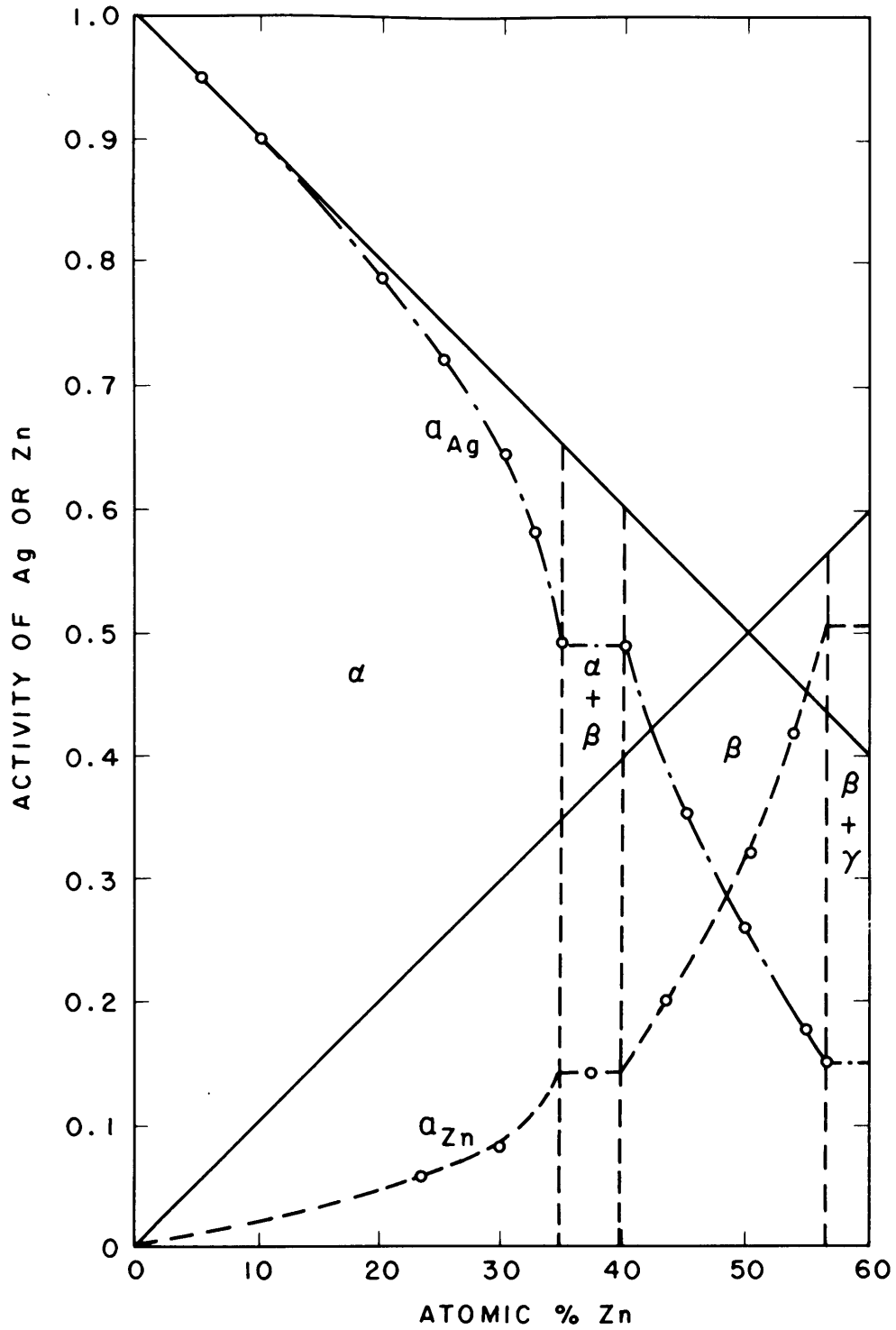
ACTIVITIES OF Ag & Zn IN Ag-Zn ALLOYS AT 620°C
(ACTIVITY OF Zn REFERRED TO LIQUID Zn)

FIGURE 7

## V. POWDERED ALLOYS

### A. Preparation of Specimens

Silver-zinc powder specimens were prepared from the same homogenized castings which were used to obtain the polycrystalline samples. Powders were filed by hand with number 4 Nicholson files from the periphery of the casting. A total of 24 hours was taken to produce about 95 grams of silver-zinc filings, 54 grams of which passed a 325 mesh (0.044 millimeter) Tyler screen. The filing was performed on a degreased vise, with clean files and clean paper to catch the filings. Iron contamination from the files was minimized by passing a permanent magnet carefully over the powders; the screens had been previously washed in benzene to remove extraneous particles. Before use, the powders were kept in stoppered bottles in an evacuated dessicator in an effort to prevent further gas adsorption and dust pick-up.

Barrett[24] points out that filing done under ordinary conditions may result in about one percent of dust, moisture, etc. being picked up. Since filing and screening was not done under argon, as he suggested, it is very likely that some dust was present.

Apparently these alloys oxidize very readily at room temperature. The purple tarnish usually observed on the casting disappeared upon a stroke of the file, but would return in a few minutes. The gray color of the first filings could be seen turning to a definite deep purple within the course of half an hour. This color change could be observed even when the filings were placed in an evacuated dessicator.

## B.  Procedure

The powder was fed into one end of the cleaned quartz tube up to the point usually occupied by the solid specimens.  The tube was gently tapped on end to pack the filings as much as possible, since at best only about 1.5 grams of the alloy filings would fill this space.  Thus the apparent volume occupied by the powder was nearly the same as that of the solid cylinder.  The tube was sealed and evacuated as before, except that the precaution of inserting a cotton plug in the vacuum line was taken.

The next day, after heating in the furnace, a light brown cloudy deposit appeared at the cold end of the tube, almost completely obscuring the droplets.  No better results were obtained by cleaning the powders initially in acetone.  Finally the procedure was adopted of preheating the powders in evacuated tubes for about 48 hours at 560° C in order to free the filings of volatile substances.  This resulted in a relatively clean surface on the quartz tube.

In order to determine the extent to which the filings were modified by this treatment, a metallographic examination was made of the filings mounted in bakelite.  The most noticeable effect was one of rounding off the sharp and jagged saw-tooth edges, leaving essentially the same over-all particle size.  They were easily separated, and showed no tendency toward sintering together.

The powder vapors exhibited an inordinate sluggishness toward evaporating and condensing at the lower temperatures as compared with the corresponding polycrystalline specimens, due no doubt to an increased
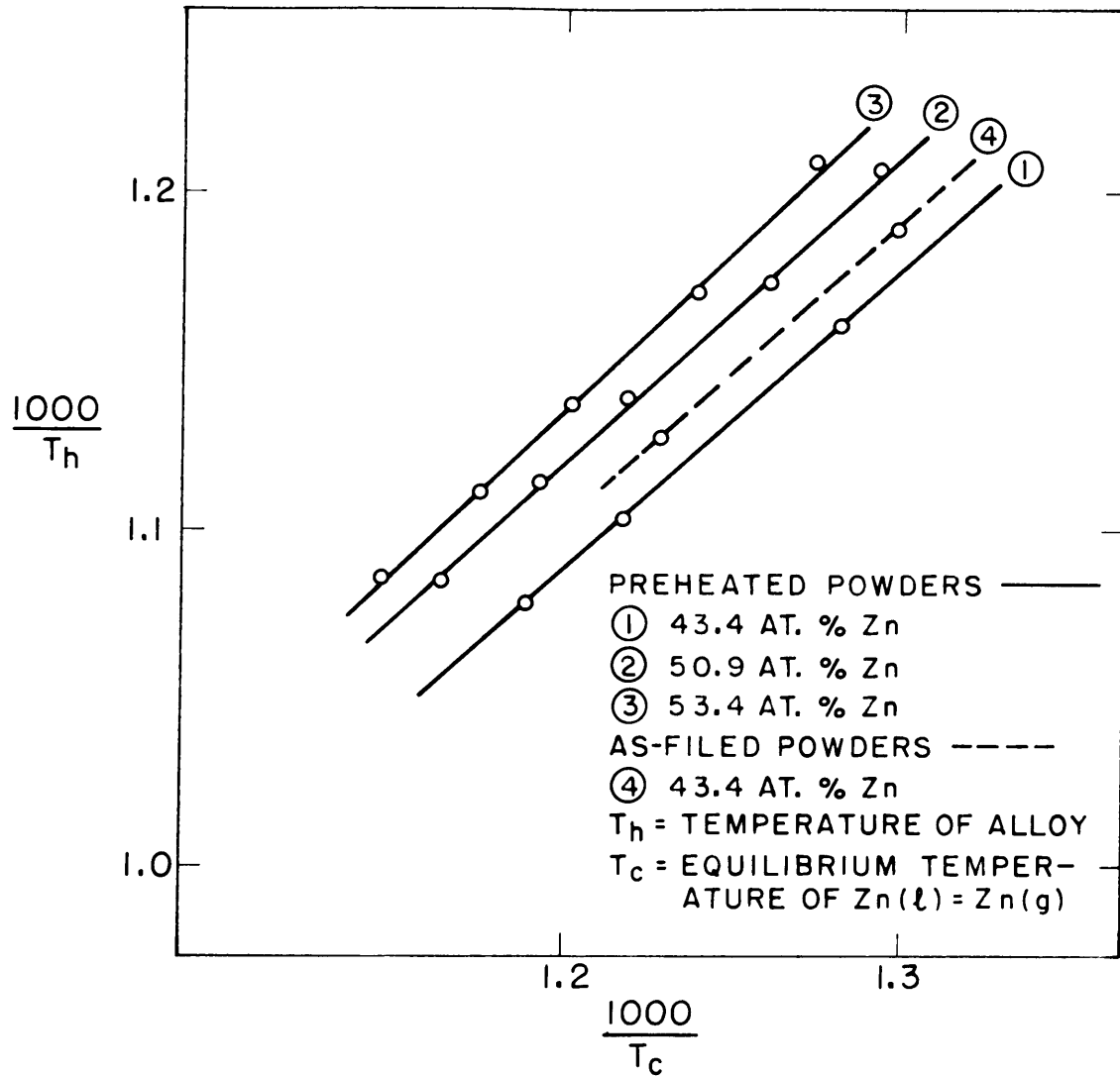
PLOT OF $\frac{1}{T_h}$ VS $\frac{1}{T_c}$ FOR POWDER SPECIMENS

FIGURE 8

oxide film on the particles. The temperature range was therefore re-
stricted to 560 - 650° C.

The experimentally determined points are tabulated in Table VII
in the Appendix and are shown in Figure 8 along with two points which
were obtained from powders which were not preheated.

## C. Discussion of Results

The most significant result obtained here is the marked increase
in pressure of the as-filed powders over both the pressures of the pre-
heated particles and the bulk alloy. The vapor pressures over the pre-
heated particles were almost identical with that over the bulk alloy of
the same composition. At 614° C there was a Zn vapor pressure of 3.50
millimeters for the raw filings as compared with 2.95 millimeters for
the bulk alloy; at 568° C, 1.26 millimeters for the raw filings com-
pared with 1.09 millimeters for the bulk alloy. Stating the results in
another way, $p'/p = 1.19$ in the first case and 1.16 in the second.
Although these points were obtained under very difficult and uncertain
conditions, the fact that they appear on a line parallel to the others
seems to indicate that the effect was real.

The effect can be most simply explained by referring to the two-
dimensional cross-sections of a typical filing shown in Figure 9.
Although here we do not have the spherically shaped particle so generally
postulated in derivations of Thompson's equation, we can still draw
qualitative conclusions between the radius and the vapor pressure. In
the sketch of the as-filed particle of Figure 9 it is seen that the
actual radii of the sharp points are much less than 0.044/2 millimeter.

AS-FILED



0.044 mm

PRE-HEATED



~0.044 mm
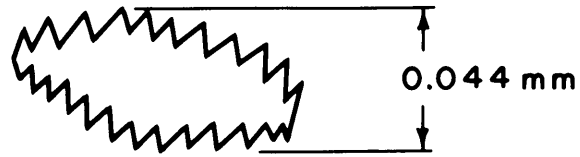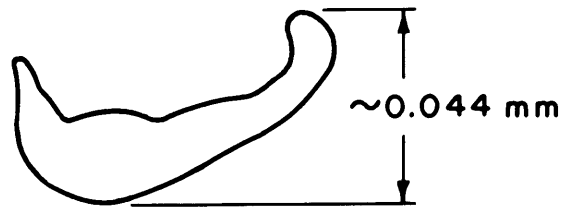
CROSS-SECTIONS OF Ag-Zn FILINGS

FIGURE 9

Small enough radii would show an increased vapor pressure, if enough were present, and this could readily be the case for the as-filed powders.

The data are summarized in Table II, and the increase in vapor pressure is compared with calculated values using the Thompson equation as modified for particles from a binary alloy. It is seen that the effective curvature of the jagged edges should be less than 0.1 micron.

## TABLE II

### Vapor Pressures of Silver-Zinc Filings

| Temperatures | Vapor Pressures of Zinc (mm) | | Ratios |
|---|---|---|---|
| (°C.) | p'(as-filed powders) | p(bulk alloy) | p'/p |
| 568 | 1.26 | 1.09 | 1.16 |
| 614 | 3.50 | 2.95 | 1.19 |

### Theoretical Ratios from the Thompson Equation

| Radius of Curvature | | Ratios |
|---|---|---|
| (cm) | (microns) | p'/p |
| 0.01 | 100 | $1.0_42$ |
| $0.0_21$ | 10 | $1.0_32$ |
| $0.0_31$ | 1 | $1.0_22$ |
| $0.0_41$ | 0.1 | 1.02 |
| $0.0_51$ | 0.01 | 1.22 |
| $0.0_61$ | $0.0_21$ | 7.40 |
| $0.0_71$ | $0.0_31$ | $5 \times 10^8$ |

(The Thompson equation, $\ln p'/p = \dfrac{2\sigma \overline{V}}{RTr}$ , was evaluated at 800° K, using $\sigma \approx 700$ ergs/cm$^2$ and $\overline{V}$, the partial molar volume of Zn in the alloy, $\approx 9.4$ cm$^3$/mole of AgZn.)

The preheated powders, as has been noted before, show as their essential difference from the as-filed powders the absence of these extremely sharp, jagged edges. The effective radii of these powders would therefore be greater, and inasmuch as only a small increase in radius is needed to render any effect of increased vapor pressure unnoticeable, the results obtained tend to this conclusion.

After making the three powder runs, the powders were again mounted in bakelite and observed under the microscope. After a maximum of eleven days in the furnace (in one case) evidence of sintering was observed. Except for a few such sintered agglomerates, the remaining loose particles still showed effectively the same over-all size.

A decided change in the compositions of these powders would not appear unlikely, considering the various treatments which they had undergone. However, subsequent chemical analysis checked remarkably well with the original analysis. The cloudy film from the as-filed particles which obscured the tube was analyzed spectroscopically, and except for strong zinc lines, only traces of silicon, nickel and copper was found in any amount (see Table III).

TABLE III

Chemical Analyses of Powdered Alloys

(Weight percent)

Before vapor pressure measurements:

| | | | |
|---|---|---|---|
| Ag: | 68.32 | 62.10 | 58.80 |
| Zn: | 31.80 | 38.16 | 41.36 |
| | 100.12 | 100.26 | 100.16 |

After vapor pressure measurements:

| | | | |
|---|---|---|---|
| Ag: | 68.27 | 61.41 | 58.96 |
| Zn: | 31.72 | 38.57 | 40.96 |
| | 99.99 | 99.98 | 99.92 |

Film formed from as-filed powders

(spectroscopic analysis):

Zn, 100-1.0%;  Ni, Si, 10-0.1%;

Cu, 1.0-0.01%; Ag, Fe, Mg,

Mn, 0.1-0.001%

## VI. SINGLE CRYSTALS

### A. Preparation of Specimens

A cylindrical AgZn single crystal with a composition of 50.7 atomic percent zinc was cut into quadrants with a jewelers handsaw. Three sections were wet-ground into cylinders which would fit into the quartz tubes. Using back-reflection methods, each crystal was oriented and ground, exposing different planes, viz., the (100), (110) and (111).

In order to remove surface cold work, electrolytic etching with a 60% orthophosphoric acid solution[25] was used. Etching was continued until the Laue back-reflection spots showed no distortion.

Apiezon black wax was used to shield the different planes; then, using a silver cyanide plating solution[26] the remaining exposed surfaces of the specimen were plated with silver. Preliminary trials revealed plating conditions which resulted in tightly adherent and dense, but somewhat rough, coatings of silver. It was assumed that the use of identical times, current densities, bath temperatures, etc. would give a plating of essentially the same thickness; however, the silver plating varied from 0.030 millimeter to 0.089 millimeter. The determination of thicknesses was made after the runs so as not to introduce cold work. A hole in the crystal for the thermocouple well was not made for the same reason. Apparently this caused no serious departures from linearity in the experimental plots.

B. Procedure

The specimens were inserted in the quartz tubes with the exposed faces toward the interior. The same experimental procedure was followed as previously described. In order to diminish the undesirable effect of zinc diffusion through the silver coating, a smaller temperature range was employed for each crystal. The plot of experimental values is shown in Figure 10 and the data are tabulated in Table VIII in the Appendix. The chemical analyses are shown in Table IV.

## TABLE IV

### Chemical Analyses of Single Crystals

(Weight percent)

Before vapor pressure measurements:

| | |
|---|---|
| Ag: | 61.57 |
| Zn: | 38.34 |
| | 99.91 |

After vapor pressure measurements:

| Outside of Crystal: | | Inside of Crystal: | |
|---|---|---|---|
| Ag: | 61.85 | Ag: | 61.43 |
| Zn: | 37.88 | Zn: | 38.54 |
| | 99.73 | | 99.97 |

(Single crystal 100)
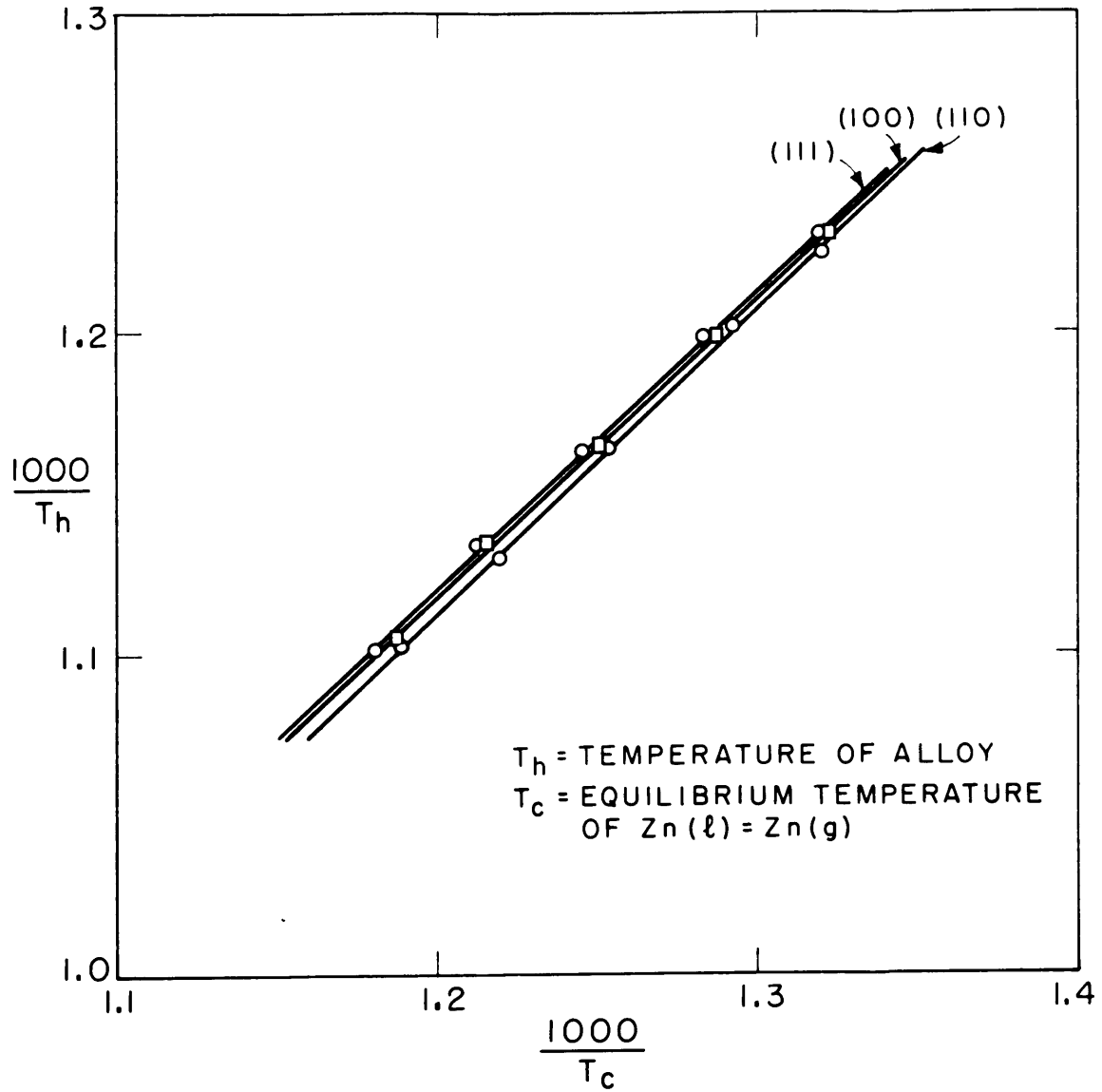
PLOT OF $\frac{1}{T_h}$ VS $\frac{1}{T_c}$ FOR 50.7 AT. % Zn SINGLE CRYSTALS

FIGURE 10

## C. Discussion of Results

Slight, but definite differences in pressure were found between the crystal faces. It was also noted that the thicker the silver plate, the lower the zinc vapor pressure. Thus it would appear that the pressures were more representative of the over-all composition than of the original unplated specimens, and that with coatings of equal thickness the zinc vapor pressures should more closely approach one another.

Diffusion of zinc would occur not only from the inside of the specimen outward through the silver plating, but also from the zinc vapor in the tube inward. Therefore, on the basis of Buckle's value of $D \approx 10^{-5}$ centimeter$^2$ per day for zinc through silver[23], we could expect somewhat more than the 0.04 percent zinc diffusing through a 0.089 millimeter layer of silver in one day. Nevertheless, no systematic trends were observed during the run which would indicate that the zinc vapor pressure was changing abnormally.

After the run the mounted and sectioned specimens showed that the original adherence of the silver plating had been maintained quite well except for a slight loosening in the (100) specimen. Two chemical analyses were made — one from filings mainly from the periphery of the specimen (61.85 percent silver) and the other from the interior (61.43 percent silver) — which averaged slightly higher than the original analysis (61.57 percent silver). This would indicate that diffusion of zinc into the silver layer had progressed considerably.

The specimens were quenched in water immediately after completion of the vapor pressure measurements in order to determine if any

recrystallization had occurred.  Only one small parasitic grain was observed in the (110) specimen upon sectioning, polishing and etching.

In any event, positive conclusions cannot be drawn from these results, since the data lie well within the limits of experimental error.

## VII.  POLYCRYSTALLINE TERNARY ALLOYS

A.  Introduction

The critical temperature for order-disorder in a 50 atomic
percent zinc silver-zinc alloy cannot be observed due to the forma-
tion of the Zeta phase upon slow cooling past 280° C.  The replace-
ment of small amounts of silver by gold suppresses the Zeta phase
and raises the critical temperature for long range ordering.  If this
critical temperature is measured as a function of gold content,
extrapolation to zero gold gives a critical temperature for AgZn of
272° C.

The study of short range order in silver-zinc alloys by x-ray
methods is possible because of the difference in scattering power
of the two atoms.  Since the transformation of quenched silver-zinc
alloys is similar to that found in $\beta'$-brass, comparison can be made
with the predictions of the Cowley theory[27] for $\beta$-brass.

Thus a knowledge of the vapor pressures of zinc over silver-
zinc-gold alloys will permit calculations of the interaction energies
from thermodynamic relations, revealing the present degree of cor-
relation between x-ray and thermodynamic data.

B.  Preparation of Specimens

A calculated amount of gold shot or wire was added to molten
silver-zinc base alloys of known composition.  The procedure was
similar to that previously described.  The dimensions of these
castings were 1/2 inch in diameter and 2 1/2 inches in length,

and they were annealed at 630° C for about six days.

Two compositions of ternary alloys were made — the compositions shown in Table V were obtained by chemical analysis of machinings from the homogenized castings.

TABLE V

Chemical Analyses of Ternary Alloys

(Weight percent)

Before vapor pressure measurements:

| | | |
|---|---|---|
| Ag: | 58.20 | 56.54 |
| Zn: | 34.50 | 30.44 |
| Au: | 7.26 | 14.00 |
| | 99.96 | 100.98 |

C. Procedure

The zinc vapor pressure measurements were made over the same temperature range as for the polycrystalline silver-zinc alloys and in the same manner. The experimental results are tabulated in Table IX in the Appendix and plotted in Figure 11.

D. Discussion of Results

The zinc vapor pressures of these two alloys were less than those obtained from silver-zinc alloys at the same temperature and with the same mole fraction of zinc. This had been anticipated, since Schneider and Schmid[11] had shown that under identical conditions liquid gold-zinc alloys had lower activities than liquid silver-zinc alloys. Hargreaves[1] measured the zinc vapor pressures of
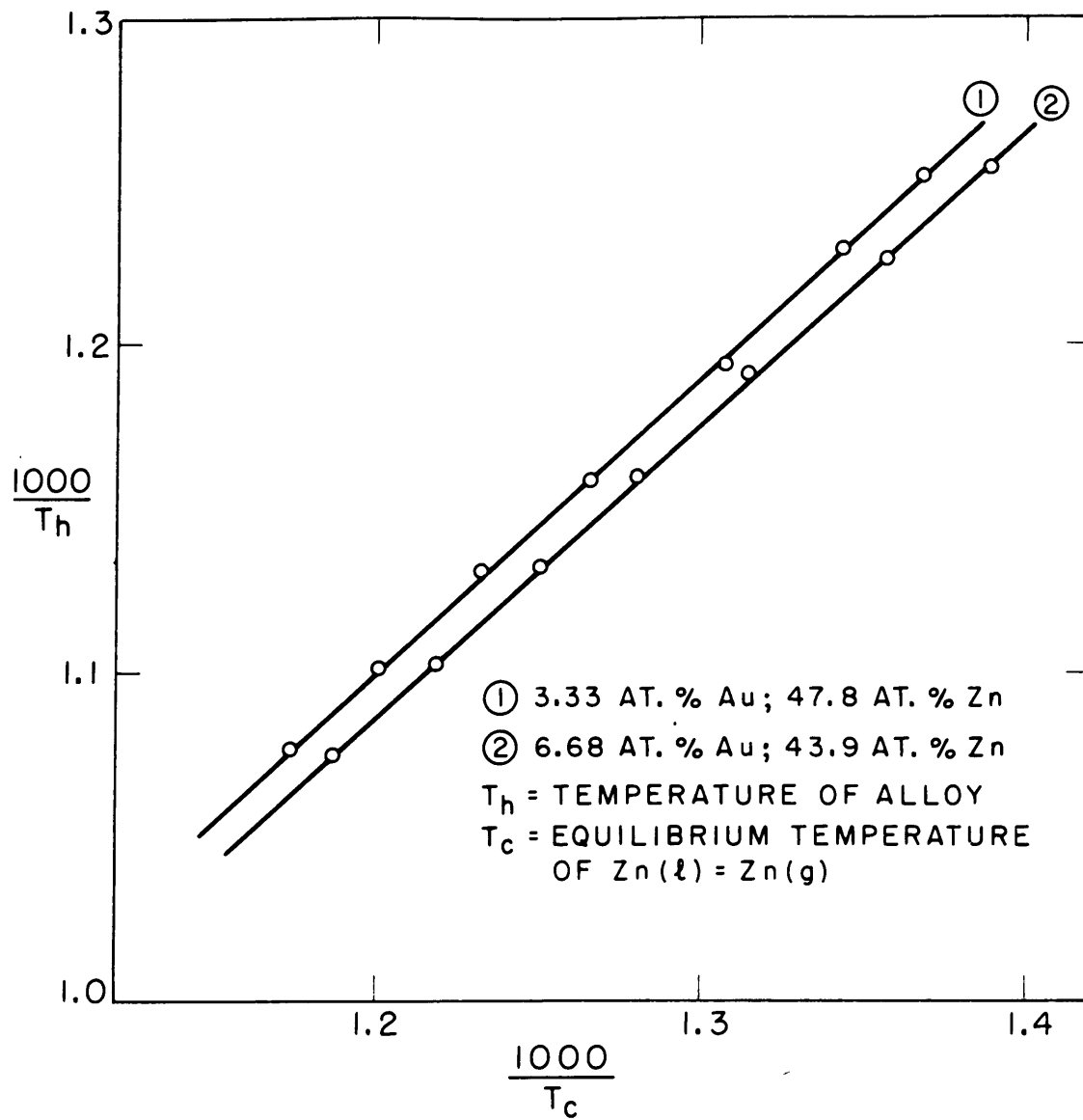
PLOT OF $\frac{1}{T_h}$ VS $\frac{1}{T_c}$ FOR AgZnAu ALLOYS

FIGURE II

nickel-copper-zinc alloys, and also found a decrease in the vapor pressures compared with corresponding copper-zinc alloys. A comparison of the activities of zinc in the binary and ternary alloys is made in Table XII in the Appendix.

Over the composition range studied, in which the composition of silver was practically constant, an unexpected effect was noted. As the fraction of the third element (gold) decreased, the difference in zinc vapor pressures between the binary and ternary alloys increased. One would rather expect that as the two compositions became more alike, so would the vapor pressures tend to approach one another.

Using Hargreaves'[1] data for nickel-copper-zinc alloys, a similar comparison was made with his alloys of constant copper content. The same behavior was also observed here — the deviation of vapor pressures became greater with decreasing amounts of nickel (see Figure 12).

In both cases this difference in vapor pressures must be approaching a maximum toward higher zinc contents, because ultimately, lower and lower amounts of the third elements (gold or nickel) must result in the two vapor pressure curves coinciding.

For $\beta$-brass, Cowley's theory[27] predicts a relation between the interaction energy, $\nu$, and the critical temperature, $T_c$, of

$$\frac{\nu}{k} = -\frac{T_c}{4} \tag{8}$$

where k = Boltzmann's constant.

Using Muldawer's[3] value of $272^\circ$ C for $T_c$ in AgZn, $N_o \nu$ should be equal to -270 calories.

AT. % Zn IN AgZn ALLOYS

| | Zn | Ag | Au (AT. %) |
|---|---|---|---|
| ① | 43.9 | 49.4 | 6.68 |
| ② | 47.8 | 48.9 | 3.33 |

| | Zn | Cu | Ni (AT. %) |
|---|---|---|---|
| ③ | 19.4 | 60.7 | 19.8 |
| ④ | 22.2 | 61.2 | 16.5 |
| ⑤ | 25.6 | 61.6 | 12.7 |
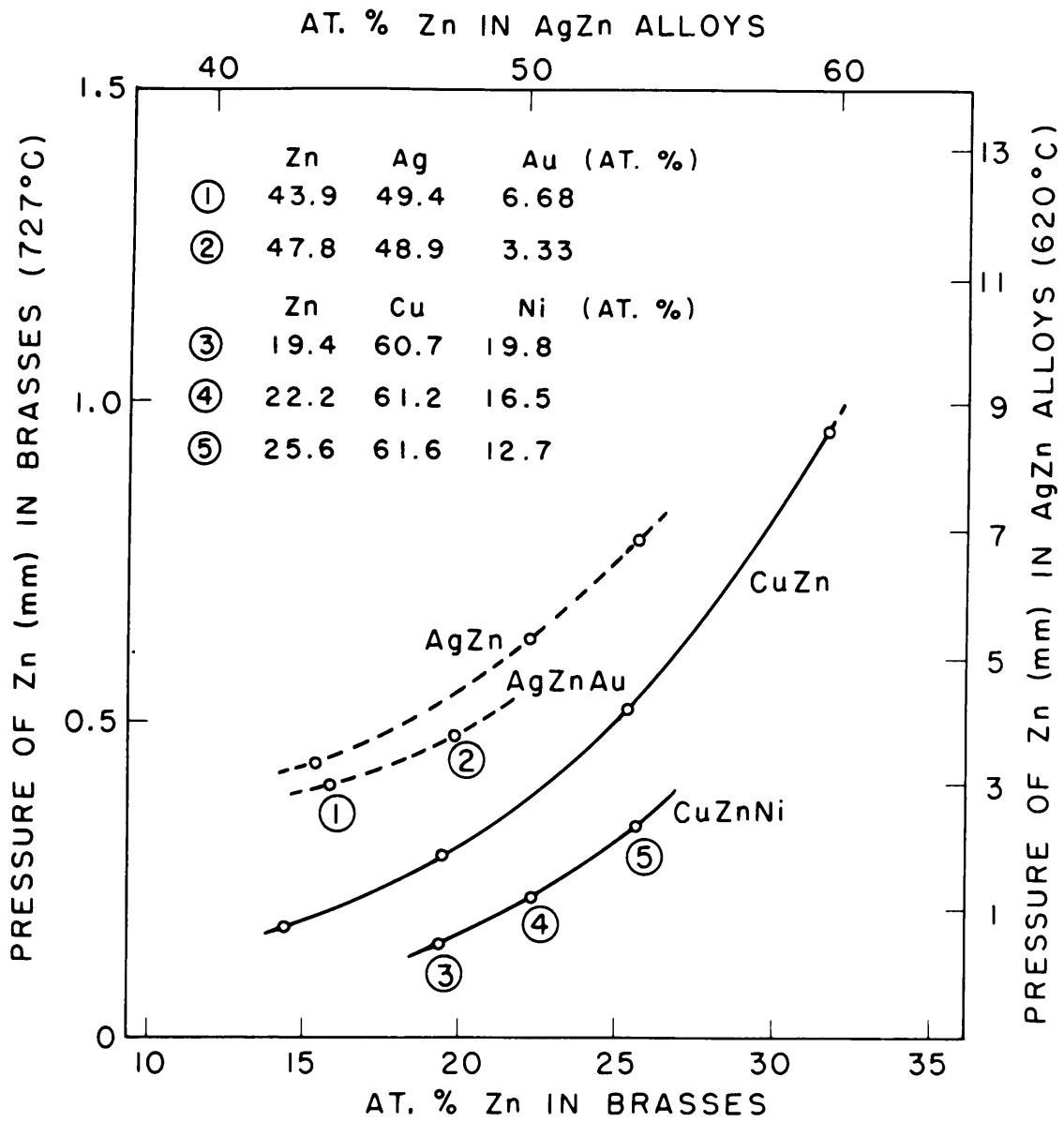
COMPARISON OF Zn VAPOR PRESSURES FROM
TERNARY AND BINARY ALLOYS

FIGURE 12

In order to check this value, a regular solution approximation,

$$\frac{Z\nu}{kT}(1-X_A)^2 = \ln \gamma_A \qquad (9)$$

where

Z = no. of nearest neighbors

$\nu$ = interaction energy = $E_{AB} - \frac{1}{2}(E_{AA} + E_{BB})$

k = Boltzmann's constant

T = temperature, °K

$X_A$ = mole fraction of A

$\gamma_A$ = activity coefficient of A,

was employed, using the activity coefficients as determined in this investigation for the 50.7 atomic percent zinc binary alloy.

Since $\gamma_{Zn}$ was known as a function of temperature, $\ln \gamma_{Zn}$ was plotted against $1/T_h$. The slope of the resulting straight line was equal to $\frac{Z\nu(1-X_{Zn})^2}{k}$ from which $N_0\nu$ could be determined.

Over a temperature range of 500-660° C, a value of $N_0\nu$ = -790 calories was obtained.

Part of this discrepancy is due to the fact that the activities have been expressed in terms of solid zinc (hexagonal close packed) whereas the $\nu$ is calculated with respect to solid zinc (body centered cubic). This change in state does not occur in zinc. However, titanium undergoes a transformation from hexagonal close packed to body centered cubic for which the change in free energy is known[28]. Applying the free energy expression for titanium

$$\Delta F° = 950 - 0.83 T \qquad (10)$$

to a hypothetical change in state, Zn(H.C.P.) = Zn (B.C.C.), enables

activities to be calculated with respect to zinc with a body centered cubic structure. Surprisingly enough, this extremely crude approximation gives a new value of $N_0 \nu = -296$ calories which compares very favorably with Cowley's value of -270 calories.

This same procedure was adopted with the 47.8 atomic percent zinc (3.33 atomic percent gold) ternary alloy, using $T_c = 318^\circ$ C from Muldawer's work[3]. Without the correction given by Equation 10, $N_0 \nu = -940$ calories while Cowley's Equation 8 predicts $N_0 \nu = -294$ calories. Using the approximation assumed in Equation 10, $N_0 \nu = -415$ calories is obtained. This change is in the right direction, but still far from a satisfactory agreement.

The possibility of any direct comparison between Cowley's theory and the activity coefficients of zinc in the ternary alloys seems improbable because of the complications introduced by the gold. However, the agreement obtained with the binary AgZn alloy is extremely encouraging and further work in systems for which the necessary data are available would seem well worth while.

# VIII. CONCLUSIONS

The activities of zinc in three solid $\beta$ silver-zinc alloys have been obtained over a temperature range of 500-660° C. In general, values obtained in this research agree quite well with previously published data for solid and liquid silver-zinc alloys. The activities of silver in silver-zinc alloys have been computed at 620° C from 100 percent silver to about 55 percent silver.

The vapor pressures for all of the alloys measured are compared in Figure 13 using the straight-line relationship between ln $p_{Zn}$ and $1/T_h$. The lines appear quite parallel to one another for alloys in the filed as well as in the bulk form, and fall in the order of increasing zinc vapor pressure from left to right. Thus it is seen for the four alloys with 43+ atomic percent zinc, for example, that the as-filed particles have the greatest vapor pressure, followed in decreasing order by the binary alloy, the preheated powders and the ternary alloy. Since the activities of zinc at any temperature are proportional to the vapor pressure over the alloys, this graph also shows the relative order with respect to activities.

A definite particle size effect was noted from the as-filed powders. The increased vapor pressures indicated a theoretical particle radius of about 0.03 micron, but there is good reason to believe that for particles with this radius of curvature the classical Thompson equation is not valid. It is more reasonable to assume that the operation of other influences (for example, a greatly disturbed

AT. % Zn
BINARY ALLOYS
① 43.4
② 50.3
③ 53.7
TERNARY ALLOYS
④ 43.9 (6.68 AT. % Au)
⑤ 47.8 (3.33 AT.% Au)
SINGLE CRYSTALS
⑥ 50.7 (110)
⑦ 50.7 (100)
⑧ 50.7 (111)
POWDER ALLOYS
⑨ 43.4
⑩ 50.9 } PRE-HEATED
⑪ 53.4
⑫ 43.4 AS FILED
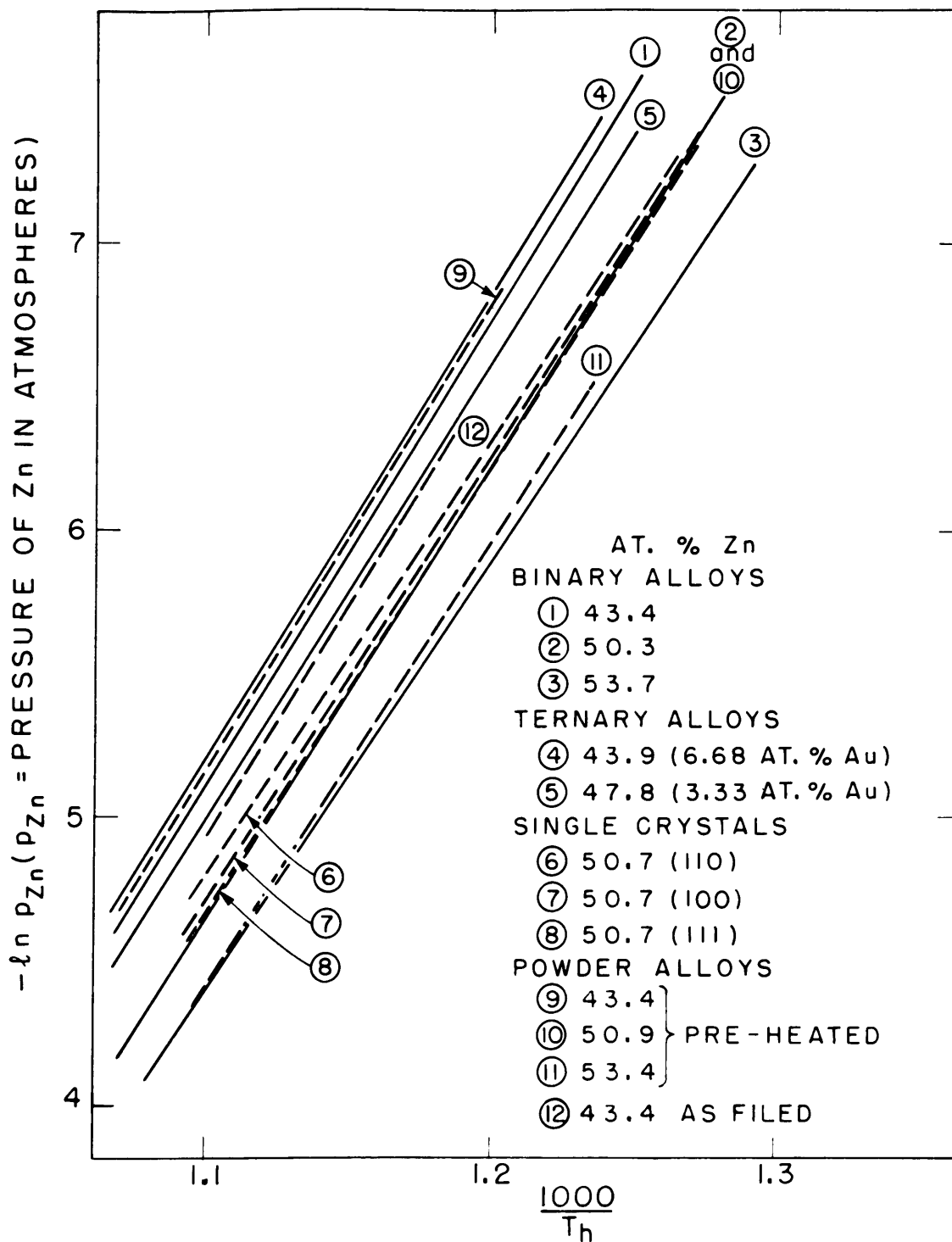
PLOT OF $\ln p_{Zn}$ VS $\frac{1}{T_h}$ FOR ALL ALLOYS

FIGURE 13

surface due to the filing operation) were responsible for the observed effect.

Encouraging agreement has been reached between both x-ray and thermodynamic data for the value of the interaction energy of AgZn. The crudity of the assumptions used in the thermodynamic treatment precludes further calculation, but the method seems hopeful for those systems for which exact data can be obtained.

# IX. REFERENCES

(1)    R. Hargreaves:  The Vapour Pressure of Zinc in Brasses,

       Jnl. Inst. of Metals, LXIV, 115 (1939).

(2)    C. E. Birchenall:  Physical Factors Affecting Order in

       Metallic Systems, Thermodynamics in Physical Metallurgy,

       Amer. Soc. for Metals, Cleveland, 158 (1950)

(3)    L. Muldawer:  X-ray Measurement of Long Range Order in

       $\beta$-AgZn, Jnl. Appl. Phys., June (1951), (To be published).

(4)    R. F. Mehl and E. L. McCandless:  Oxide Films on Iron,

       Trans. A.I.M.E., 125, 546, (1937)

(5)    R. P. Johnson:  Construction of Filament Surfaces,

       Phys. Review, 54, 459 (1938): 53, 766 (1938).

(6)    C. Wagner:  Part III in G. Masing's Handbuch der

       Metallphysik, Leipzig (1940).  (J. W. Edwards, Ann

       Arbor, Mich.)

(7)    J. Chipman and J. F. Elliott:  The Thermodynamics of

       Liquid Metallic Solutions, Thermodynamics in Physical

       Metallurgy, Amer. Soc. for Metals, Cleveland, 102 (1950).

(8)    L. L. Seigle and D. Turnbull:  The Measurement of Activity

       Coefficients of Metal Solutions, Gen. Elect. Research Lab.

       Schenectady, N. Y. (1948)

(9)    C. E. Birchenall and C. H. Cheng:  The Vapor Pressures of

       Zinc and Cadmium over some of Their Silver Alloys,

       Trans. A.I.M.E., 185, 428 (1949).

(10) F. Weibke and O. Kubaschewski: Thermochemie der Legierungen, Berlin (1943) (J. W. Edwards, Ann Arbor, Mich.).

(11) A. Schneider and H. Schmid: The Vapor Pressures of Zinc and Cadmium over Their Binary Liquid Alloys with Copper, Silver and Gold, Ztsch. Elektrochem., 48, 627 (1942).

(12) S. L. Bigelow and H. M. Trimble: The Relation of Vapor Pressure to Particle Size, Jnl. Phys. Chem., 31, 1798 (1927).

(13) N. K. Adam: The Physics and Chemistry of Surfaces, The Clarendon Press, Oxford (1938).

(14) E. K. Rideal: An Introduction to Surface Chemistry, The University Press, Cambridge, England (1930).

(15) R. Shuttleworth: The Surface Tension of Solids, Proc. Phys. Soc., Sec. A, 63, Part 5, No. 365 A, 444 (1950).

(16) F.. O. Koenig: On the Thermodynamic Relation Between Surface Tension and Curvature, Jnl. Chem. Phys., 18, 449 (1950).

(17) W. Ostwald: Ztsch. Physik. Chemie, 18, 159 (1895); 34, 495 (1900).

(18) G. A. Hulett: Ztsch. Physik. Chemie, 37, 385 (1901); 47, 357 (1904).

(19) Freundlich: Kapillarchemie, 63 (1922).

(20) S. Glasstone: Thermodynamics for Chemists, D. Van Nostrand, New York, (1947)

(21) K. K. Kelley: Contributions to the Data on Theoretical Metallurgy, Bur. of Mines Bull. 383, 108 (1935).

(22)  Metals Handbook, Amer. Soc. for Metals, Cleveland, 1155 (1948).

(23)  H. Bückle:  The Diffusion Process for Noble-Metal Platings, II,

Metalforsch., 1, 108 (1946).

(24)  C. S. Barrett:  Structure of Metals, McGraw-Hill Book Co.,

New York, 184 (1943).

(25)  L. W. Larke and E. B. Wicks:  Electrolytic Polishing and

Etching of some Al-Ag-Alloys, Metallurgia, 41, 172, Jan. (1950).

(26)  Metals Handbook, Amer. Soc. for Metals, Cleveland, 1107 (1948).

(27)  J.M. Cowley:  An Approximate Theory of Order in Alloys,

Phys. Rev., 77, 669 (1950).

(28)  K. K. Kelley:  Contributions to the Data on Theoretical

Metallurgy, Bur. of Mines Bull. 476, 192 (1949).

# APPENDIX A

## TABLE VI

Experimental Temperatures for Binary Alloys

| 43.4 at.% Zn | | | 50.3 at.% Zn | | | 53.7 at.% Zn | | |
|---|---|---|---|---|---|---|---|---|
| $T_h(^\circ C)$ | $T_c(^\circ C)$ | $\Delta T$ | $T_h(^\circ C)$ | $T_c(^\circ C)$ | $\Delta T$ | $T_h(^\circ C)$ | $T_c(^\circ C)$ | $\Delta T$ |
| 527.0 | 451.5 | 75.5 | 525.2 | 468.3 | 56.9 | 523.2 | 482.0 | 41.2 |
| 540.5 | 465.6 | 74.9 | 539.7 | 485.5 | 54.2 | 537.7 | 496.5 | 41.2 |
| 560.5 | 484.5 | 76.0 | 565.0 | 506.9 | 58.1 | 562.9 | 518.7 | 44.2 |
| 586.7 | 509.4 | 77.3 | 587.8 | 531.8 | 56.0 | 587.8 | 544.2 | 43.6 |
| 610.5 | 531.4 | 79.1 | 608.3 | 548.7 | 59.6 | 608.6 | 562.5 | 46.1 |
| 634.4 | 551.5 | 82.9 | 633.0 | 573.0 | 60.0 | 630.7 | 584.0 | 46.7 |
| 658.0 | 573.4 | 84.6 | 655.5 | 595.2 | 60.3 | 654.9 | 606.8 | 48.1 |

(Check Points)

| 43.4 at.% Zn | | | 50.3 at.% Zn | | | 53.7 at.% Zn | | |
|---|---|---|---|---|---|---|---|---|
| 586.0 | 508.7 | 77.3 | 539.0 | 485.5 | 53.5 | 555.2 | 512.0 | 43.2 |

## TABLE VII

### Experimental Temperatures for Powdered Alloys

(Pre-heated)

| 43.4 at.% Zn | | | 50.9 at.% Zn | | | 53.4 at.% Zn | | |
|---|---|---|---|---|---|---|---|---|
| $T_h(^{\circ}C)$ | $T_c(^{\circ}C)$ | $\Delta T$ | $T_h(^{\circ}C)$ | $T_c(^{\circ}C)$ | $\Delta T$ | $T_h(^{\circ}C)$ | $T_c(^{\circ}C)$ | $\Delta T$ |
| 588.7 | 506.9 | 81.8 | 556.5 | 500.4 | 56.1 | 554.6 | 511.5 | 43.1 |
| 633.9 | 548.9 | 85.0 | 579.5 | 520.0 | 59.5 | 581.5 | 533.6 | 47.9 |
| 655.5 | 568.4 | 87.1 | 605.2 | 547.5 | 57.7 | 606.5 | 559.0 | 47.5 |
| | | | 624.4 | 565.7 | 58.7 | 626.5 | 578.8 | 47.7 |
| | | | 649.0 | 587.0 | 62.0 | 648.0 | 600.9 | 47.1 |

### Powdered Alloys (as-filed)

#### 43.4 at.% Zn

| | | |
|---|---|---|
| 567.9 | 496.5 | 71.4 |
| 613.8 | 541.2 | 72.6 |

## TABLE VIII

Experimental Temperatures for Single Crystals

| 50.7 at.% Zn(100) | | | 50.7at.% Zn(110) | | | 50.7at.% Zn(111) | | |
|---|---|---|---|---|---|---|---|---|
| $T_h(^{\circ}C)$ | $T_c(^{\circ}C)$ | $\Delta T$ | $T_h(^{\circ}C)$ | $T_c(^{\circ}C)$ | $\Delta T$ | $T_h(^{\circ}C)$ | $T_c(^{\circ}C)$ | $\Delta T$ |
| 539.0 | 483.0 | 56.0 | 543.8 | 484.4 | 59.4 | 539.5 | 484.5 | 55.0 |
| 561.0 | 503.5 | 57.5 | 559.5 | 500.5 | 59.0 | 561.8 | 505.5 | 56.3 |
| 585.4 | 526.0 | 59.4 | 586.7 | 524.7 | 62.0 | 587.2 | 529.8 | 57.4 |
| 608.8 | 549.6 | 59.2 | 612.5 | 546.5 | 66.0 | 609.5 | 552.0 | 57.5 |
| 631.4 | 569.0 | 62.4 | 634.0 | 568.4 | 65.6 | 635.0 | 573.8 | 61.2 |

## TABLE IX

Experimental Temperatures for Ternary Alloys

| 43.9 at.% Zn (6.68 at.% Au) | | | 47.8 at.% Zn (3.33 at.% Au) | | |
|---|---|---|---|---|---|
| $T_h$(°C) | $T_c$(°C) | $\Delta T$ | $T_h$(°C) | $T_c$(°C) | $\Delta T$ |
| 525.0 | 446.5 | 78.5 | 526.0 | 457.2 | 68.8 |
| 542.6 | 463.6 | 79.0 | 540.5 | 471.0 | 69.5 |
| 566.8 | 487.5 | 79.3 | 564.5 | 491.3 | 73.2 |
| 589.4 | 507.6 | 81.8 | 590.8 | 516.5 | 74.3 |
| 610.4 | 526.4 | 84.0 | 611.3 | 537.7 | 73.6 |
| 634.0 | 546.9 | 87.1 | 634.5 | 557.3 | 77.2 |
| 657.5 | 568.8 | 88.7 | 655.4 | 578.4 | 77.0 |

## APPENDIX B

## Calculation of Activities and Tabulation of Data

The temperatures obtained experimentally were not used directly, but the best straight line through them was used to get $\frac{1}{T_b}$ (at 20° C intervals) and the corresponding values of $\frac{1}{T_c}$.

These temperatures were substituted in the free energy equation for the change in state, Zn (l) = Zn (g)

$$\Delta F^o = 30,902 + 6.03 T \log T + 0.275 \times 10^{-3} T^2 - 45.03 T \tag{1}$$

which was rearranged to give

$$-\ln p_{Zn} = 15,550.5(\tfrac{1}{T}) + 3.0347 \log T + 1.3838 \times 10^{-4} T - 22.66, \tag{2}$$

since $\Delta F^o = -RT \ln p_{Zn}$ ($p_{Zn}$ = pressures in atmospheres).

The activity of Zn in the alloy, referred to liquid Zn as the standard state, is

$$a_{Zn} = \frac{p_{Zn(alloy)}}{p_{Zn}^{\bullet}} \tag{3}$$

The activity of Zn in the alloy, referred to solid Zn as the standard state, was obtained from the free energy equation for the change in state, Zn (s) = Zn (g)

$$\Delta F^o = 31,392 + 0.64 T \log T + 1.35 \times 10^{-3} T^2 - 31.17 T \tag{4}$$

which was used in the form

$$-\ln p_{Zn}^o = 15,797.1(\tfrac{1}{T}) + 0.32206 \log T + 6.7935 \times 10^{-4} T - 15.685. \tag{5}$$

The $p_{Zn}^o$ obtained from Equation 5, substituted in Equation 3, gives the activity of Zn in the alloy, referred to solid Zn.

The data are tabulated below for the binary and ternary alloys.

## TABLE X

### Activity Data for Binary Alloys

(Activities of Zn referred to Liquid Zn)

43.4 at. % Zn

| $T_h$(°C) | $-\ln p$ | $p$(atm.) | $T_c$(°K) | $\dfrac{1000}{T_c}$ | $\log T_c$ | $-\ln a$ |
|---|---|---|---|---|---|---|
| 500 | 8.255 | 0.00026 | 701.03 | 1.4265 | 2.8457 | 1.9314 |
| 520 | 7.722 | 0.00045 | 719.52 | 1.3898 | 2.8570 | 1.8687 |
| 540 | 7.216 | 0.00073 | 738.03 | 1.3550 | 2.8681 | 1.8093 |
| 500 | 6.735 | 0.0012 | 756.56 | 1.3218 | 2.8789 | 1.7528 |
| 580 | 6.278 | 0.0019 | 775.11 | 1.2901 | 2.8894 | 1.6989 |
| 600 | 5.842 | 0.0029 | 793.68 | 1.2600 | 2.8997 | 1.6475 |
| 620 | 5.427 | 0.0044 | 812.26 | 1.2311 | 2.9097 | 1.5985 |
| 640 | 5.031 | 0.0065 | 830.86 | 1.2036 | 2.9195 | 1.5515 |
| 660 | 4.653 | 0.0095 | 849.48 | 1.1772 | 2.9292 | 1.5067 |

50.3 at. % Zn

| $T_h$(°C) | $-\ln p$ | $p$(atm.) | $T_c$(°K) | $\dfrac{1000}{T_c}$ | $\log T_c$ | $-\ln a$ |
|---|---|---|---|---|---|---|
| 500 | 7.742 | 0.00043 | 718.80 | 1.3912 | 2.8566 | 1.4185 |
| 520 | 7.218 | 0.00073 | 737.95 | 1.3551 | 2.8680 | 1.3650 |
| 540 | 6.721 | 0.0012 | 757.12 | 1.3208 | 2.8792 | 1.3144 |
| 560 | 6.249 | 0.0019 | 776.33 | 1.2881 | 2.8901 | 1.2662 |
| 580 | 5.800 | 0.0030 | 795.55 | 1.2570 | 2.9007 | 1.2206 |
| 600 | 5.372 | 0.0046 | 814.81 | 1.2273 | 2.9111 | 1.1769 |
| 620 | 4.964 | 0.0070 | 834.10 | 1.1989 | 2.9212 | 1.1352 |
| 640 | 4.575 | 0.0105 | 853.41 | 1.1718 | 2.9312 | 1.0955 |
| 660 | 4.203 | 0.015 | 872.76 | 1.1458 | 2.9409 | 1.0573 |

TABLE X (Continued)

53.7 at. % Zn

| $T_h(^oC)$ | $-\ln p$ | p(atm.) | $T_c(^oK)$ | $\frac{1000}{T_c}$ | log $T_c$ | $-\ln a$ |
|---|---|---|---|---|---|---|
| 500 | 7.341 | 0.00065 | 733.37 | 1.3636 | 2.8653 | 1.017 |
| 520 | 6.843 | 0.0011 | 752.30 | 1.3293 | 2.8764 | 0.990 |
| 540 | 6.372 | 0.0017 | 771.23 | 1.2966 | 2.8872 | 0.965 |
| 560 | 5.923 | 0.0026 | 790.15 | 1.2656 | 2.8977 | 0.940 |
| 580 | 5.498 | 0.0041 | 809.04 | 1.2360 | 2.9080 | 0.919 |
| 600 | 5.090 | 0.0061 | 828.02 | 1.2077 | 2.9180 | 0.895 |
| 620 | 4.704 | 0.0090 | 846.91 | 1.1807 | 2.9278 | 0.875 |
| 640 | 4.334 | 0.018 | 865.82 | 1.1550 | 2.9374 | 0.855 |
| 660 | 3.981 | 0.0185 | 884.78 | 1.1302 | 2.9468 | 0.835 |

## TABLE XI

### Activity Data for Ternary Alloys

(Activity of Zn referred to liquid Zn)

43.9 at. % Zn (6.68 at. % Au)

| $T_h(^\circ C)$ | $-\ln p$ | p(atm.) | $T_c(^\circ K)$ | $\dfrac{1000}{T_c}$ | log $T_c$ | $-\ln a$ |
|---|---|---|---|---|---|---|
| 500 | 8.3507 | 0.00024 | 697.83 | 1.4330 | 2.8438 | 2.0268 |
| 520 | 7.8165 | 0.00040 | 716.17 | 1.3963 | 2.8550 | 1.9632 |
| 540 | 7.3097 | 0.00066 | 734.53 | 1.3614 | 2.8660 | 1.9030 |
| 560 | 6.8281 | 0.0011 | 752.91 | 1.3282 | 2.8767 | 1.8456 |
| 580 | 6.3701 | 0.0017 | 771.30 | 1.2965 | 2.8872 | 1.7911 |
| 600 | 5.9338 | 0.0026 | 789.70 | 1.2663 | 2.8975 | 1.7389 |
| 620 | 5.5180 | 0.0040 | 808.12 | 1.2374 | 2.9075 | 1.6893 |
| 640 | 5.1210 | 0.0060 | 826.56 | 1.2098 | 2.9173 | 1.6416 |
| 660 | 4.7420 | 0.0088 | 845.00 | 1.1834 | 2.9269 | 1.5962 |

47.8 at. % Zn (3.33 at. % Au)

| $T_h(^\circ C)$ | $-\ln p$ | p(atm.) | $T_c(^\circ K)$ | $\dfrac{1000}{T_c}$ | log $T_c$ | $-\ln a$ |
|---|---|---|---|---|---|---|
| 500 | 8.1140 | 0.00030 | 795.84 | 1.4168 | 2.8487 | 1.7901 |
| 520 | 7.5900 | 0.00050 | 724.45 | 1.3804 | 2.8600 | 1.737 |
| 540 | 7.0828 | 0.00085 | 743.08 | 1.3458 | 2.8710 | 1.6761 |
| 560 | 6.6056 | 0.0013 | 761.73 | 1.3128 | 2.8818 | 1.6231 |
| 580 | 6.1520 | 0.0021 | 780.38 | 1.2814 | 2.8923 | 1.5730 |
| 600 | 5.7197 | 0.0032 | 799.07 | 1.2515 | 2.9026 | 1.5248 |
| 620 | 5.3079 | 0.0050 | 817.77 | 1.2228 | 2.9126 | 1.4792 |
| 640 | 4.9147 | 0.0074 | 836.49 | 1.1955 | 2.9225 | 1.4353 |
| 660 | 4.5392 | 0.011 | 855.23 | 1.1693 | 2.9321 | 1.3934 |

## TABLE XII

### Comparison of Activities of Zn in Binary and Ternary Alloys

(Activity of Zn referred to liquid Zn)

| | 500 | 520 | 540 | 560 | 580 | 600 | 620 | 640 | 660 | (°C) |
|---|---|---|---|---|---|---|---|---|---|---|
| Binary Alloy, 43.4 at. % Zn | | | | | | | | | | |
| | .145 | .154 | .163 | .173 | .182 | .192 | .202 | .211 | .221 | |
| Ternary Alloy, 43.9 at. % Zn | | | | | | | | | | |
| | .131 | .140 | .149 | .158 | .166 | .175 | .185 | .194 | .204 | |
| Binary Alloy, 50.3 at. % Zn | | | | | | | | | | |
| | .242 | .255 | .268 | .281 | .295 | .308 | .321 | .334 | .347 | |
| Ternary Alloy, 47.8 at. % Zn | | | | | | | | | | |
| | .167 | .176 | .187 | .196 | .208 | .217 | .227 | .238 | .249 | |

(Activities of Zn referred to solid Zn)

| | 500 | 520 | 540 | 560 | 580 | 600 | 620 | 640 | 660 | (°C) |
|---|---|---|---|---|---|---|---|---|---|---|
| Binary Alloy, 50.3 at. % Zn | | | | | | | | | | |
| | .214 | .220 | .225 | .230 | .235 | .240 | .245 | .250 | .254 | |
| Ternary Alloy, 47.8 at. % Zn | | | | | | | | | | |
| | .148 | .151 | .156 | .160 | .165 | .170 | .174 | .177 | .181 | |

## TABLE XIII

### Vapor Pressure Data for Solid and Liquid Zn

| $T_h(^oC)$ | $T_h(^oK)$ | $\dfrac{1000}{T_h(^oK)}$ | $\log T_h(^oK)$ | Zn(l)=Zn(g) | | Zn(s)=Zn(g) | |
|---|---|---|---|---|---|---|---|
| | | | | $-\ln p^o$ | p(atm) | $-\ln p^o$ | p(atm) |
| 500 | 773.2 | 1.2933 | 2.8883 | 6.3239 | .0018 | 6.2013 | .0020 |
| 520 | 793.2 | 1.2607 | 2.8994 | 5.8533 | .0029 | 5.7033 | .0033 |
| 540 | 813.2 | 1.2297 | 2.9102 | 5.4067 | .0045 | 5.2305 | .0053 |
| 560 | 833.2 | 1.2002 | 2.9208 | 4.9825 | .0068 | 4.7812 | .0085 |
| 580 | 853.2 | 1.1721 | 2.9311 | 4.5790 | .0102 | 4.3537 | .013 |
| 600 | 873.2 | 1.1452 | 2.9411 | 4.1949 | .015 | 3.9465 | .019 |
| 620 | 893.2 | 1.1196 | 2.9510 | 3.8287 | .022 | 3.5581 | .028 |
| 640 | 913.2 | 1.0951 | 2.9606 | 3.4794 | .031 | 3.1875 | .041 |
| 660 | 933.2 | 1.0716 | 2.9700 | 3.1458 | .044 | 2.8334 | .059 |

## TABLE XIV

### Activities of Zn in All Alloys

(Referred to liquid Zn)

| | 500 | 520 | 540 | 560 | 580 | 600 | 620 | 640 | 660 (°C) |
|---|---|---|---|---|---|---|---|---|---|
| **Binary Alloys** | | | | | | | | | |
| 43.4 at. % Zn | .145 | .154 | .163 | .173 | .182 | .192 | .202 | .211 | .221 |
| 50.3 at. % Zn | .242 | .255 | .268 | .281 | .295 | .308 | .321 | .334 | .347 |
| 53.7 at. % Zn | .361 | .371 | .381 | .390 | .399 | .408 | .417 | .425 | .434 |
| **Powdered Alloys** | | | | | | | | | |
| 43.4 at. % Zn | | | | .161 | .170 | .179 | .189 | .197 | .207 |
| 50.9 at. % Zn | | | .270 | .282 | .295 | .305 | .318 | .330 | .342 |
| 53.4 at. % Zn | | | .360 | .373 | .385 | .396 | .409 | .420 | .432 |
| **Single Crystals** | | | | | | | | | |
| 50.7 at. % Zn (100) | | .260 | .270 | .280 | .290 | .300 | .310 | .319 | |
| 50.7 at. % Zn (110) | | .246 | .254 | .262 | .269 | .276 | .284 | .291 | |
| 50.7 at. % Zn (111) | | .266 | .276 | .287 | .298 | .309 | .318 | .330 | |
| **Ternary Alloys** | | | | | | | | | |
| 43.9 at. % Zn | .131 | .140 | .149 | .158 | .166 | .175 | .185 | .194 | .204 |
| 47.8 at. % Zn | .167 | .176 | .187 | .196 | .208 | .217 | .227 | .238 | .249 |

## TABLE XV

### Activity Coefficients of Zn in all Alloys

(Activity of Zn referred to liquid Zn)

| | 500 | 520 | 540 | 560 | 580 | 600 | 620 | 640 | 660 (°C) |
|---|---|---|---|---|---|---|---|---|---|
| **Binary Alloys** | | | | | | | | | |
| 43.4 at. % Zn | .334 | .355 | .376 | .399 | .420 | .443 | .466 | .486 | .509 |
| 50.3 at. % Zn | .481 | .507 | .532 | .559 | .586 | .612 | .638 | .664 | .689 |
| 53.7 at. % Zn | .672 | .690 | .709 | .726 | .743 | .761 | .775 | .791 | .808 |
| **Powdered Alloys** | | | | | | | | | |
| 43.4 at. % Zn | | | | .371 | .392 | .413 | .436 | .454 | .477 |
| 50.9 at. % Zn | | | .530 | .554 | .580 | .599 | .625 | .648 | .672 |
| 53.4 at. % Zn | | | .675 | .699 | .721 | .742 | .766 | .787 | .810 |
| **Single Crystals** | | | | | | | | | |
| 50.7 at. % Zn (100) | | .513 | .532 | .552 | .572 | .591 | .611 | .629 | |
| 50.7 at. % Zn (110) | | .485 | .501 | .517 | .530 | .544 | .560 | .574 | |
| 50.7 at. % Zn (111) | | .525 | .544 | .566 | .588 | .610 | .627 | .650 | |
| **Ternary Alloys** | | | | | | | | | |
| 43.9 at. % Zn | .298 | .319 | .339 | .360 | .378 | .399 | .421 | .442 | .464 |
| 47.8 at. % Zn | .349 | .368 | .391 | .410 | .435 | .454 | .475 | .498 | .520 |

TABLE XVI

Activities and Activity Coefficients of Ag at 620° C

in Ag-Zn Alloys

Mole fraction of Ag

   1.00 .950 .900 .800 .750 .700 .675 .652 .604 .550 .500 .450 .433

Activity of Ag

   1.00 .950 .900 .786 .721 .644 .582 .490 .490 .353 .260 .175 .150

Activity Coefficients of Ag

   1.00 1.00 .999 .984 .960 .920 .862 .752 .812 .642 .519 .389 .346

# APPENDIX C

## Calculation of Partial Molar Heats of Formation

The relative partial molar heats of formation were calculated for all alloys from the relation

$$\frac{\partial \ln a_{Zn}}{\partial \left(\frac{1}{T_h}\right)} = \frac{\Delta \bar{H}}{R} \tag{1}$$

where $a_{Zn}$ = activity of Zn (referred to liquid Zn) in Ag-Zn alloys

$\Delta \bar{H}$ = the relative partial molar enthalpy of Zn in Ag-Zn

R = The gas constant

$T_h$ = Temperature of the alloy, °K.

The slope of the straight line resulting when ln a is plotted vs. $1/T_h$ gives the values of $\Delta \bar{H}$.

Figure A-1 shows the plot of ln a vs. $1/T_h$ for all alloys and Table XVII gives the calculated values of $\Delta \bar{H}$ from this research as well as from Birchenall and Cheng[9].
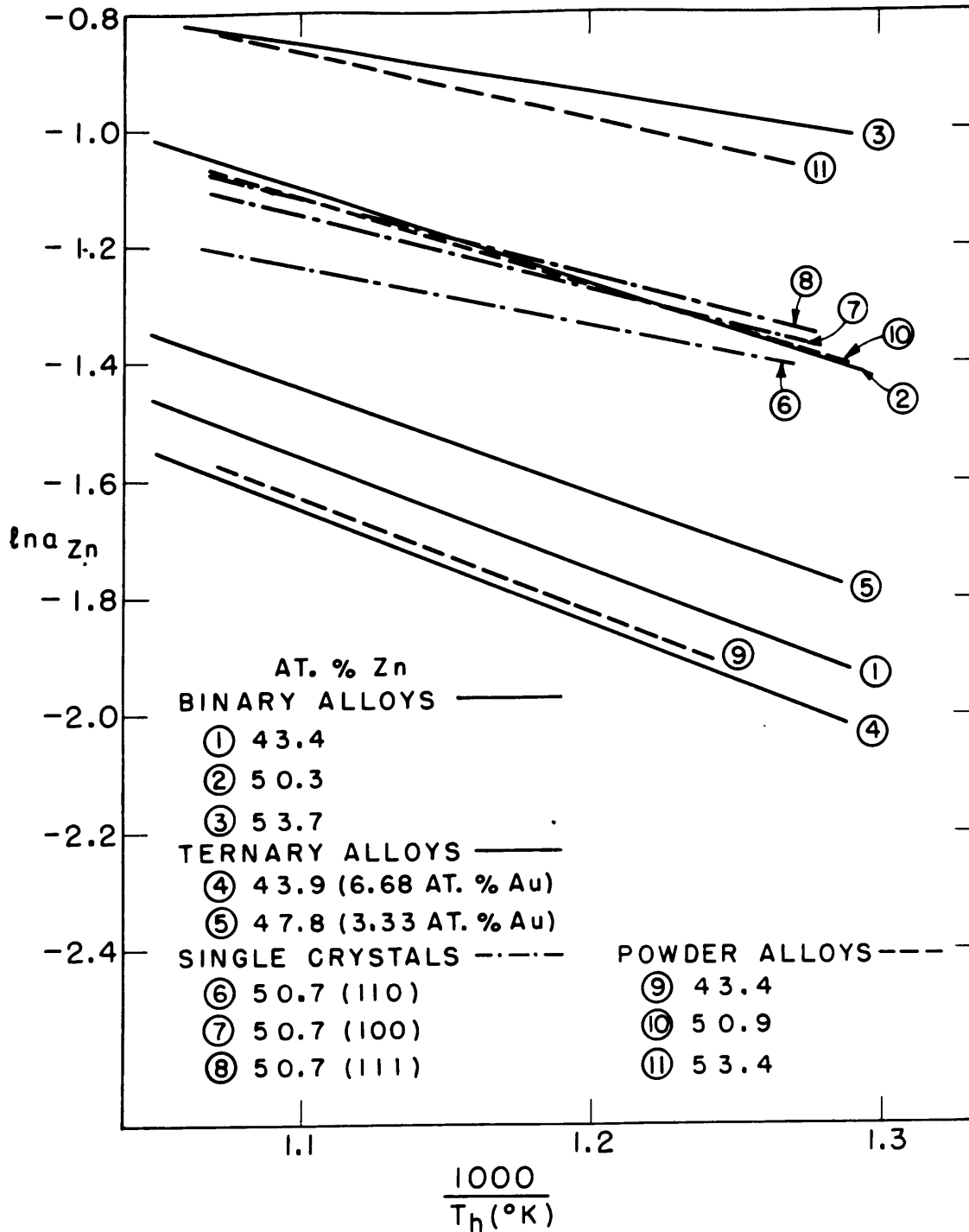
PLOT OF $\ln a_{Zn}$ VS $\frac{1}{T_h}$ FOR $\beta$ Ag Zn ALLOYS

FIGURE A-1

## TABLE XVII

### Partial Molar Heats of Formation

| Binary Alloys | $\Delta \overline{H}$ (cal.) |
|---|---|
| 43.4 at. % Zn | -3810 |
| 50.3 at. % Zn | -3240 |
| 53.7 at. % Zn | -1630 |

| Powdered Alloys | |
|---|---|
| 43.4 at. % Zn | -3840 |
| 50.9 at. % Zn | -2970 |
| 53.4 at. % Zn | -2290 |

| Single Crystals | |
|---|---|
| 50.7 at. % Zn (100) | -2470 |
| 50.7 at. % Zn (110) | -1960 |
| 50.7 at. % Zn (111) | -2580 |

| Ternary Alloys | |
|---|---|
| 43.9 at. % Zn (6.68 at. % Au) | -3860 |
| 47.8 at. % Zn (3.33 at. % Au) | -3560 |

Calculated from Birchenall and Cheng[9]

| Binary Alloys | |
|---|---|
| 7.34 at. % Zn | -2420 |
| 10.54 at. % Zn | -2850 |
| 17.33 at. % Zn | -4920 |
| 23.45 at. % Zn | -5170 |
| 29.65 at. % Zn | -6050 |
| 54.87 at. % Zn | -2055 |

APPENDIX D

Activities of Ag at $620^\circ$ C in Ag-Zn Alloys

Using Gibbs-Duhem Relationship

By combining the Gibbs-Duhem equation in the form $N_1 d\mu_1 + N_2 d\mu_2 = 0$,

with the expression for the chemical potential, viz., $\mu_i = \mu_i^\circ + RT \ln a_i$,

it is seen that for a binary solution,

$$N_1 d \ln a_1 + N_2 d \ln a_2 = 0, \qquad (1)$$

where $N_1$ and $N_2$ are the mole fractions of solvent and solute,

respectively.

Since $N_1 + N_2 = 1$ for a binary mixture, $dN_1 + dN_2 = 0$, and

hence,

$$N_1 \frac{dN_1}{N_1} + N_2 \frac{dN_2}{N_2} = 0, \qquad (2)$$

that is,

$$N_1 d \ln N_1 + N_2 d \ln N_2 = 0. \qquad (3)$$

If this is subtracted from Equation 1 the result is

$$N_1 d \ln \frac{a_1}{N_1} + N_2 d \ln \frac{a_2}{N_2} = 0$$

$$d \ln \frac{a_1}{N_1} = -\frac{N_2}{N_1} d \ln \frac{a_2}{N_2}. \qquad (4)$$

Upon integrating and converting the logarithms it is found that

$$\log \frac{a_1}{N_1} - \log \frac{a_1'}{N_1'} = -\int_{N_2'}^{N_2} \frac{N_2}{N_1} d \log \frac{a_2}{N_2}. \qquad (5)$$

The fraction $N_2/N_1$ becomes infinite at $N_2 = 1$, and integration

to this limit involves an extrapolation to infinity.

Using the relationship

$$\int u \, dv = uv - \int v \, du \tag{6}$$

Equation 5 can be rewritten to obtain

$$\log \frac{a_1}{N_1} - \log \frac{a_1'}{N_1'} = \int_{N_2'}^{N_2} \frac{\log \gamma_2'}{N_1^2} dN_2 - \left[ \frac{\log \gamma_2'}{N_1^2} N_2 N_1 \right]_{N_2'}^{N_2} \tag{7}$$

In this case the function within the integral apparently approaches

a finite limit when $N_2$ approaches unity.

Compositions of the phase boundaries at $620°$ C (obtained from

the phase diagram) and their corresponding values of $\gamma_{Zn}'$ are given

in Table XVIII.

### TABLE XVIII

#### Compositions and Activity Coefficients

#### of Phase Boundaries at 620° C

| Composition | $\gamma_{Zn}'$ |
|---|---|
| $\alpha(\beta)* = $ 34.77 at. % Zn | 0.415 |
| $\beta(\alpha) = $ 39.63 at. % Zn | 0.362 |
| $\beta(\gamma) = $ 56.70 at. % Zn | 0.90 |

\* ( $\alpha(\beta)$ is the composition of $\alpha$ in equilibrium with $\beta$ , etc.)


Activity coefficients for Zn at $620°$ C in the $\alpha$-field were ob-

tained from data given by Birchenall and Cheng[9]. The activity

coefficients obtained from this investigation were used in the $\beta$-field.

They are listed in Table XIX.

## TABLE XIX

### Activity Coefficients of Zn at 620° C in Ag-Zn Alloys

#### $\alpha$-Field

| Composition | $\gamma_{Zn}$ |
|---|---|
| 7.34 at. % Zn | 0.186 |
| 10.53 at. % Zn | 0.225 |
| 17.33 at. % Zn | 0.239 |
| 23.45 at. % Zn | 0.240 |
| 29.65 at. % Zn | 0.274 |
| 37.15 at. % Zn | 0.415 ($\alpha$) and 0.362 ($\beta$) |

#### $\beta$-Field

| | |
|---|---|
| 43.4 at. % Zn | 0.466 |
| 50.3 at. % Zn | 0.638 |
| 53.7 at. % Zn | 0.775 |

In making this calculation over the $\alpha$-field, the lower limit becomes zero. Equation 7 can now be written

$$\log \gamma_{Ag} = \int_0^{N_{Zn}} \frac{\log \gamma_{Zn}}{N_{Ag}^2} dN_{Zn} - \frac{\log \gamma_{Zn}}{N_{Ag}^2} N_{Zn} N_{Ag} \tag{8}$$

The value of $\log \gamma_{Ag}$ $\alpha(\beta) = -0.1238$, obtained from Equation 8, gives $\log \gamma_{Ag}$ $\beta(\alpha) = -0.090$, since the activity of Ag in the two-phase region remains constant.

In the $\beta$ -field Equation 7 becomes

$$\left(log\, \gamma'_{Ag}\right)_{N_{Zn}} = \int_{N_{Zn}=.396}^{N_{Zn}} \frac{log\,\gamma'_{Zn}}{N^2_{Ag}}\, dN_{Zn} - \left(\frac{log\,\gamma'_{Zn}}{N^2_{Ag}} N_{Zn} N_{Ag}\right)_{N_{Zn}} + \left(\frac{log\,\gamma'_{Zn}}{N^2_{Ag}} N_{Zn} N_{Ag} + log\,\gamma'_{Ag}\right)_{N_{Zn}=.396} \quad (9)$$

where the last term in parenthesis is constant and equal to -0.289

-0.090 = -0.379.

The data used in obtaining the activity coefficients of Ag

at 620° C for different compositions are assembled in Table XX.

Figure A-2 shows a plot of (log $\gamma'_{Zn}/N^2_{Ag}$ ) vs. $N_{Zn}$ , from which areas

were measured with a planimeter.

## TABLE XX

### Data for the Gibbs-Duhem Integration

| $N_{Zn}$ | $\gamma_{Zn}$ | $\log \gamma_{Zn}$ | $N_{Ag}$ | $N_{Ag}^2$ | $N_{Zn}N_{Ag}$ | $\dfrac{\log \gamma_{Zn}}{N_{Ag}^2}(N_{Zn}N_{Ag})$ | $\displaystyle\int_0^{N_{Zn}}\dfrac{\log \gamma_{Zn}}{N_{Ag}^2}(dN_{Zn})$ | | $\log \gamma_{Ag}$ | $\log \gamma_{Ag}$ | $\gamma_{Ag}$ | $a_{Ag}$ |
|---|---|---|---|---|---|---|---|---|---|---|---|---|
| **From $N_{Zn}=0$** | | | | | | | | | | | | |
| 0 | .204 | -.690 | 1.0 | 1.0 | 0 | 0 | 0 | | 0 | 0 | 1 | 1 |
| .05 | .205 | -.688 | .95 | .905 | .0475 | -.0361 | -.0360 | | .0001 | .0001 | 1 | .95 |
| .10 | .209 | -.680 | .90 | .810 | .090 | -.0755 | -.0756 | | -.0001 | .9999-1 | .999 | .90 |
| .20 | .228 | -.642 | .80 | .640 | .160 | -.1605 | -.1672 | | -.0067 | .9933-1 | .984 | .786 |
| .25 | .246 | -.609 | .75 | .564 | .188 | -.2015 | -.2192 | | -.0177 | .9823-1 | .960 | .721 |
| .30 | .277 | -.557 | .70 | .490 | .210 | -.239 | -.2752 | | -.0362 | .9638-1 | .920 | .644 |
| .325 | .317 | -.499 | .675 | .457 | .219 | -.239 | -.3032 | | -.0642 | .9358-1 | .862 | .582 |
| .348 | .415 | -.382 | .652 | .426 | .227 | -.203 | -.3268 | | -.1238 | .8762-1 | .752 | .490 |
| **From $N_{Zn}=0.396$** | | | | | | | | $\log \gamma_{Ag}'$ | $\log \gamma_{Ag}'-.379$ | | | |
| .396 | .362 | -.441 | .604 | .365 | .239 | -.289 | 0 | .289 | -.090 | .910-1 | .812 | .490 |
| .45 | .500 | -.301 | .55 | .303 | .248 | -.246 | -.0590 | .187 | -.192 | .808-1 | .642 | .353 |
| .50 | .632 | -.199 | .50 | .250 | .250 | -.199 | -.1044 | .0946 | -.2844 | .7156-1 | .519 | .260 |
| .55 | .818 | -.087 | .45 | .203 | .248 | -.106 | -.1368 | -.0308 | -.4098 | .5902-1 | .389 | .175 |
| .567 | .900 | -.046 | .433 | .188 | .245 | -.0598 | -.1420 | -.0822 | -.4612 | .5388-1 | .346 | .150 |
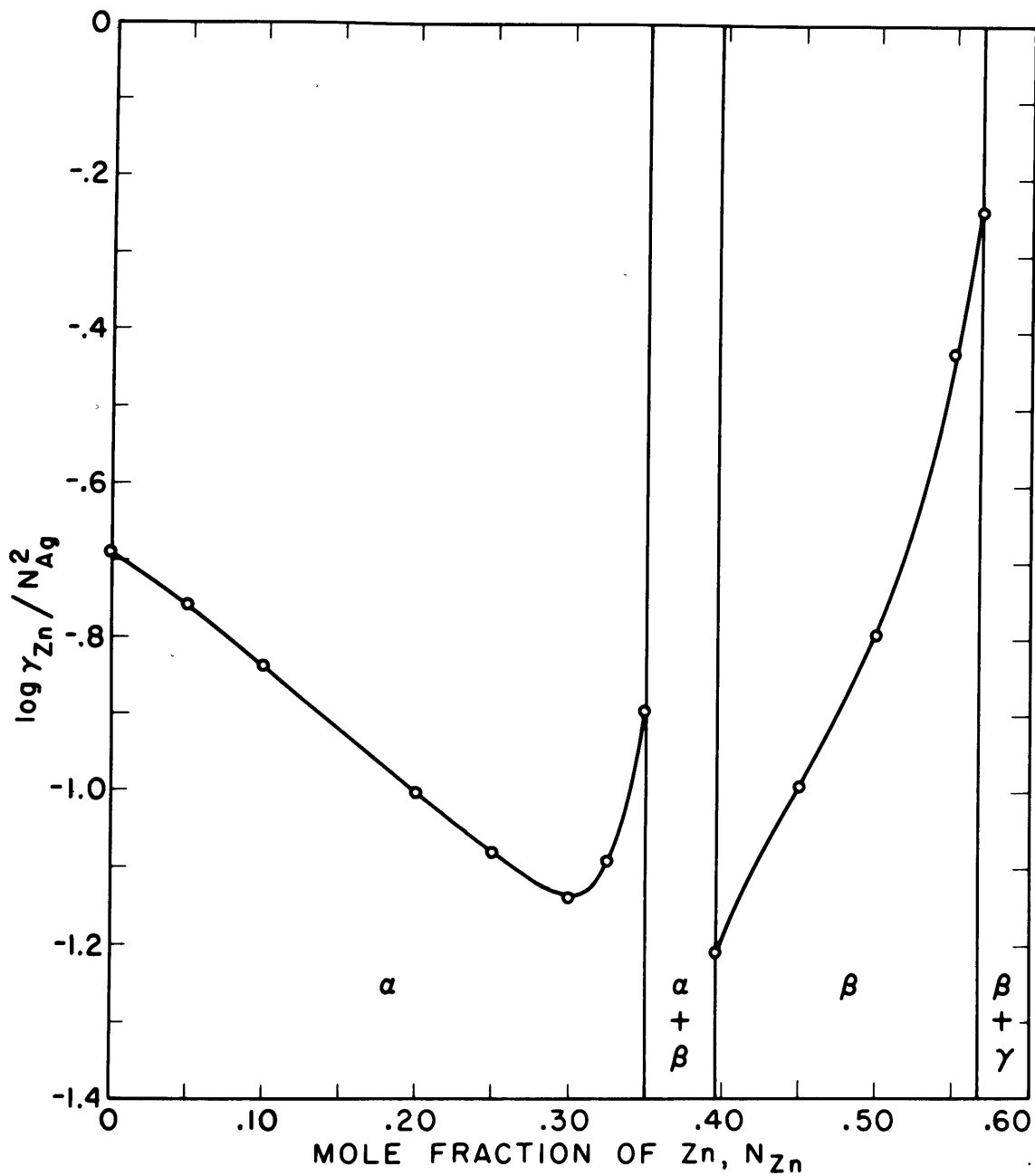
PLOT FOR GIBBS-DUHEM INTEGRATION AT 620°C

$$\log \gamma_1 - \log \gamma_1' = \int_{N_2'}^{N_2} \frac{\log \gamma_2}{N_1^2} \, dN_2 - \left[ \frac{\log \gamma_2}{N_1^2} N_2 N_1 \right]_{N_2'}^{N_2}$$

FIGURE A-2